Lancaster University

Study of the Effects of the Cannabinoids Anandamide and Cannabidiol on the feeding processes of *Tetrahymena pyriformis*

Charou Jaisswar
Student ID: 32171241

December 2019

Masters by Research Project Thesis

Supervised by Dr Jackie Parry and Dr Karen L. Wright

Declaration

This thesis is entirely my own work and has not been submitted in full or in part for the award of a higher degree at any other educational institution.

No sections of this thesis have been published.

Word count: 23,091

Table of Contents

Abstract

The regulation and physiological management of feeding behaviour, appetite and fullness in humans, and many other multicellular organisms, is governed by the pathways involved in the Endocannabinoid system (ECS). This complex system comprises lipid endocannabinoids e.g. Anandamide (AEA), that bind to cannabinoid receptors (e.g. CB1 and CB2), together with the enzymes involved in cannabinoid generation and hydrolysis. The ECS can also be stimulated by the plant cannabinoids (phytocannabinoids) such as Δ9-tetrahydrocannabidiol (Δ9-THC) and cannabidiol (CBD) which are found in *Cannabis sativa*.

This study examined the effects exogenous of AEA and CBD on prey ingestion and food vacuole formation in the ciliate *Tetrahymena pyriformis* when feeding on an indigestible fluorescent cyanobacterium *Synechococcus*. Both AEA and CBD affected the ciliate feeding by inducing a lag; AEA having a shorter lag (*ca*. 36 min) in comparison to CBD (*ca*. 60 min). When ingestion resumed, AEA-treated cells fed at the same rate as the Control cells whereas CBD-treated cells had elevated ingestion rates (hyperphagia). The mechanism behind this is currently unknown but it does not appear to involve a cessation of food vacuole trafficking and defecation. It was also considered unlikely to be due to vacuole membrane recycling and the formation of phagocytic cups as the cellular machinery for this is very similar to that required for vacuole trafficking, which is unaffected by AEA and CBD. The study therefore hypothesised that: AEA and CBD completely stops prey capture but that pre-existing vacuoles are trafficked and defecated as normal and membrane is recycled to the cytostome where it accumulates. A lag of 60 min would allow the accumulation of more membrane than a 30 min lag and is the possible reason as to why ingestion rates after the former are higher.

This study provides a basis for future research into the effects of CBD and AEA on the feeding capture processes of protists as well as their potential targets. Since protists do not possess the usual cannabinoid receptors associated with the human ECS future work might elucidate the ancestral targets of these cannabinoids together with their function in single cells.

Glossary

AA	Arachidonic acid
2-AG	2-Arachidonoylglycerols
2-AcGs	2-acylglycerols
2-O-AG	2-O-acylglycerol
AEA	*N*-arachidonoyl ethanolamine, Anandamide
AMT	AEA membrane transporter
ATP	Adenosine triphosphate
BG11	Blue green 11 broth
BLAST	Basic Local Alignment Search Tool
cAMP	Cyclic adenosine monophosphate
CB1	Cannabinoid Receptor 1
CB2	Cannabinoid Receptor 2
CBD	Cannabidiol
CBD-A	Cannabidolic acid
CBG	Cannabigerolic acid
CNS	Central Nervous System
cGMP	Cyclic guanosine monophosphate
CNS	Central Nervous System
CORVERT	Class C core vacuole/endosome tether
COX-2	Cyclooxygenase-2
DAG	Diacylglycerol
DAGLα	Diacylglycerol lipase α
DAPI	4,6- Diaminide-2-phenylindole dihydrochloride
EEA	Eicosenoylethanolamine
EEA1	Early endosomal antigen 1
ECS	Endocannabinoid System
FAAH	Fatty acid amide hydrolase
FFAs	Free Fatty Acids
Gal/GalNAc	Galactose- and N-acetyl-d-galactosamine
GlcNAc	N-Acetyl-D-glucosamine
GLEA	*N*-γ-linolenoylethanolamine

GPCR	G protein- coupled receptor
GPR55	G protein-coupled receptor 55
HMM	Heavy Meromyosin
HOPS	Homotypic fusion and vacuole sorting
IC_{50}	Half maximal inhibitory concentration
IR	Ingestion Rate
LAMP 1/2	Lysosomal- associated membrane protein 1/2
LB	Lysogeny broth
LEA	*N*-linoleoylethanolamine
LOX	Lipoxygenase
LPS	Lipopolysaccharides
MAGL	Monoacylglycerol lipase
MAPK	Mitogen- activated protein kinase
MIC	Minimum inhibitory concentration
NADPH	Nicotinamide adenine dinucleotide phosphate
NAE	N-Acyl Ethanolamines
NAPE	N- arachidonoyl phosphatidylethanolamine
NSF	N-ethylmaleimide Sensitive Factor
OEA	*N*- Oleoylethanolamine
ONE WAY ANOVA	The one-way analysis of variance
PAMPs	Pathogen-Associated MolecularPatterns
PEA	*N*-Palmitoylethanolamine
PGH_2	Prostaglandin H_2
PPAR	Peroxisome proliferator- activated receptor
PI3K	Phosphoinositide 3- kinase
PIK3 VPs34	Class III phosphatidylinositol 3- kinase vacuolar protein sorting 34
PIP3	Phosphatidylinositol 3- phosphate
PKA/B/C	Protein Kinase A/ B/C
PLC	Phospholipase C
PRR	Pattern recognition receptors
RAB5/7	Rabaptin-5/7
Rho	Rhodopsin
ROS	Reactive oxygen species

SEA	*N*- stearoylethanolamine
SEM	Standard Error of Mean
SNAREs	Soluble NSF protein receptors
TRPV1	Transient receptor potential vanilloid type 1
TD	Transmembrane Domains
THC-A	Tetrahydracannabonolic acid
VFR	Vacuole Formation Rate
VGCC	Voltage gated calcium channel
VPT	Vacuole Passage Time
Δ9-THC	Delta- 9- Tetrahydrocannabinol
5-HT1A	Hydroxytryptamine serotonin receptors

1. Introduction

1.1 The human endocannabinoid system

The endocannabinoid system (ECS) is a ubiquitous neuromodulatory system which plays a vital role in controlling regulatory functions throughout the body, i.e., central nervous, cardiovascular, immune and gastrointestinal systems (Marzo et al., 2004). It governs the regulation of systematic processes such as learning, memory, pain sensation, sleep, immune response, addiction, as well as the control of appetite/metabolism and digestion (Aizpurua-Olaizola et al., 2017). The ECS is often referred to as a "broad-spectrum modulator" (Aizpurua-Olaizola et al., 2017) because it has many components which, through interaction, contribute to the functional versatility of this system (Maccarrone et al., 2015). The components include endogenous cannabinoids (Section 1.2), the receptors they bind to (Section 1.4), along with the enzymes that synthesise and degrade the cannabinoids (Section 1.3) (Aizpurua-Olaizola et al., 2017).

1.2 Cannabinoids

Cannabinoids are biologically active long chain lipids (Kendall and Yudowski, 2017; Zou and Kumar, 2018) which function as ligands for receptors in mammals, that are primarily G-protein coupled receptors (Pertwee, 1997; Zou and Kumar, 2018). Non-synthetic cannabinoids can be classified into groups; phytocannabinoids and endogenous cannabinoids (Bilici, 2014).

1.2.1 Phytocannabinoids

Cannabinoids derived from plants are known as Phytocannabinoids (Lambert and Fowler, 2005). The most widely known and researched phytocannabinoids are delta-9-tetrahydrocannabinol (Δ9-THC) and Cannabidiol (CBD), from the plant *Cannabis sativa* (Pertwee, 2015; Maroon and Bost, 2018) (Figure 1.1). Cannabis contains over 421 chemical compounds out of which more than 60 cannabinoids have been isolated (Mechoulam, 2005; Appendino et al., 2011) that may have antagonistic or synergistic characteristics relevant to their pharmacological use (Izzo, 2001).

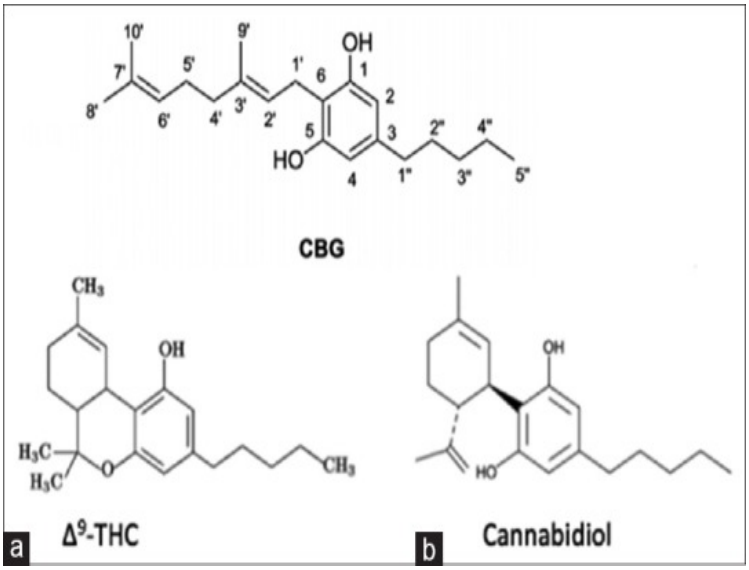

Figure 1.1: The biochemical structure of Δ9-THC, CBD and cannabigerolic acid (CBG). Both Δ9-THC and CBD are synthesized from CBG (common precursor) as tetrahydracannabonolic acid (THC-A) and cannabidolic acid (CBD-A). THC-A and CBD-A are produced directly through cannabis growth, whereas the conversion to Δ9-THC and CBD occurs when cannabis is heated e.g. for smoking or vaporising, as this causes THC-A and CBD-A to decarboxylate (Maroon and Bost, 2018).

Extracts of cannabis have been extensively used for medical purposes (Appendino et al., 2011) such as; anti-inflammatory, anti-convulsant, antinociceptive and antiemetic (Mechoulam, 1986; Iversen, 2000), targeting diseases such as gastrointestinal disorders (Grinspoon and Bakalar, 1997; Izzo, 2001), Alzheimer's disease and multiple sclerosis (MS) (Maroon and Bost, 2018). However, Δ9-THC and CBD have different side-effects concerning human feeding, i.e., the psychoactive THC enhances feeding causing subjects to have the 'munchies' (Soria-Gómez et al., 2014; Roberts et al., 2019), whereas the non-psychoactive CBD decreases appetite (Iffland and Grotenhermen, 2017). Being non-psychoactive, medicinal trials of CBD have increased as over the years and it has been shown to alleviate diabetes, depression and anxiety (Bakas et al., 2017) as well as aid in the reduction of pain in inflammatory conditions such as arthritis, and can also be used to decrease seizures in epilepsy and other psychotic symptoms (Pacher, 2006; Devinsky et al., 2014).

1.2.2 Endogenous cannabinoids (Endocannabinoids)

Endogenous cannabinoids are composed of derivatives of unsaturated fatty acids, and their main function in the ECS involves operating as endogenous ligands for cannabinoid receptors (Habayeb et al., 2002). Anandamide (AEA) was the first endogenous cannabinoid to be isolated (Devane et al., 1992). The uterus contains the highest amount of AEA in mammals, and there is more recent evidence of its role in reproduction (Schmid et al., 1997; Habayeb et al., 2002). Furthermore, AEA has been found to demonstrate various effects in

the nervous system via modulating interactions with neurotransmitters, affecting brain activities (Di Marzo et al., 1998; Habayeb et al., 2002). Research on rodents has indicated that AEA can inhibit memory consolidation (Castellano et al., 1997; Habayeb, et al., 2002), as well as hinder working memory overall (Mallet and Beninger, 1996; Habayeb et al., 2002). AEA has also been shown to have analgesic properties (Mechoulam et al., 1995) and prevent motor coordination (Di Marzo et al., 1998; Habayeb et al., 2002).

Another endogenous endocannabinoid, which acts on cannabinoid receptors, was discovered three years after AEA, i.e. 2- Arachidonoyglycerol (2-AG) (Mechoulam et al., 1995). 2-AG was first isolated within the canine gut and rat brain and in both of these organs, the concentration of this endocannabinoid was greater than that of AEA (Mechoulam et al., 1995; Stella, et al., 1997; Waku and Sugiura, 2003).

1.3 Biosynthetic and degradation enzymes

2-AG and AEA are both produced "on-demand" through biosynthetic pathways (Bisogno et al., 2001). Both AEA and 2-AG are classified as N-acylethanolamines (NAEs) and were discovered to act as endogenous lipids in hypoxic myocardium by Epps et al. (1979).

It has been established that the synthesis of AEA is a two-step process (Figure 1.2). The first step involves the generation of its membrane precursor named N-arachidonoyl phosphatidylethanolamine (NAPE) (Di Marzo et al., 1994). This process is catalysed by a calcium dependent N-acyltransacylase (NAT), which plays an essential part in the transferring of arachidonic acid (AA) from the sn-1 position of the 1,2-sn-di-arachidonylphosphatidylcholine to the amino group of the hydroxyethyl of phosphatidylethanolamine which entails the formation of NAPE (Basavarajappa, 2007). After NAPE undergoes a cleavage governed by a NAPE specific phospholipase D (NAPE-PLD) forming AEA and phosphatic acid (Natarajan et al., 1981; Schmid et al., 1983; Di Marzo et al., 1994) (Figure 1.2).

The hydrolysis and degradation of AEA to AA and ethanolamine is mediated by the enzyme fatty acid amide hydrolase (FAAH) (Deutsch and Chin, 1993; Cravatt et al., 1996) (Figure 1.2). The first report of a similar enzyme activity to FAAH was described to by Schmid et al. (1985)

who observed the hydrolysis of saturated and monosaturated NAEs in rat liver. Following this Deutch and Chin (1993) isolated FAAH in the N18TG2 neuroblastoma cells, where they first observed this enzyme's activity of converting AEA to AA. However, it was not until 1996, when Cravette et al. purified the hydrolysis activity of FAAH in rat liver membrane, that FAAH was named and recognised for its action in the ECS. The metabolism of AEA is also known to be mediated by cyclooxygenase-2 (COX-2), cytochrome P450 and lipoxygenase (LOX) (Basavarajappa, 2007a).

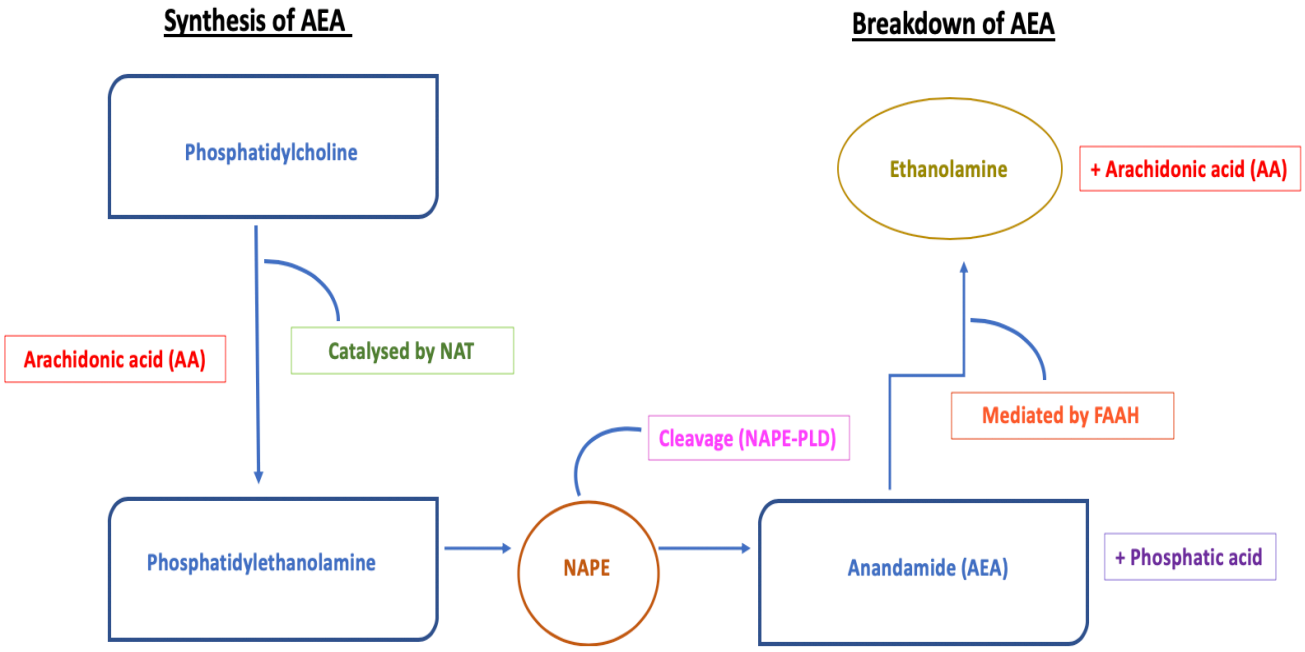

Figure 1.2: AEA is synthesised on demand by formation and hydrolysis of N-arachidonoyl phosphatidylethanolamine (NAPE). 1) NAPE is hydrolysed through the transfer of arachidonic acid (AA) also known as an acyl group, from the sn-1 position of the phosphatidylcholine to the amino group of the hydroxyethyl of phosphatidylethanolamine. This reaction is catalysed by N-acyltransacylase (NAT). 2) NAPE then undergoes cleavage mediated by N-arachidonoyl phosphatidylethanolamine specific phospholipase D (NAPE-PLD). This leads to the formation of AEA and phosphatic acid. When no longer required, AEA is degraded mainly by fatty acid amide (FAAH) to ethanolamine and arachidonic acid. This breakdown process mainly occurs in the endoplasmic reticulum of the cell.

2-AG is synthesized in neurones by two possible pathways, one of which involves phospholipase C (PLC) governed hydrolysis of membrane phospholipids that leads to the production of diacylglycerol (DAG) which is then converted to 2-AG mediated by the activity of diacylglycerol lipase (DAGL) (Prescott and Majerus, 1983; Sugiura et al., 1995). On the other hand, DAG may be produced by the hydrolysis of phosphatidic acid mediated by Mg^{2+} and Ca^{2+} dependent phosphohydrolase activity followed by the same conversion process to 2-AG as the first pathway (Waku and Sugiura, 2003; Bisogno et al., 2008) (Figure 1.3).

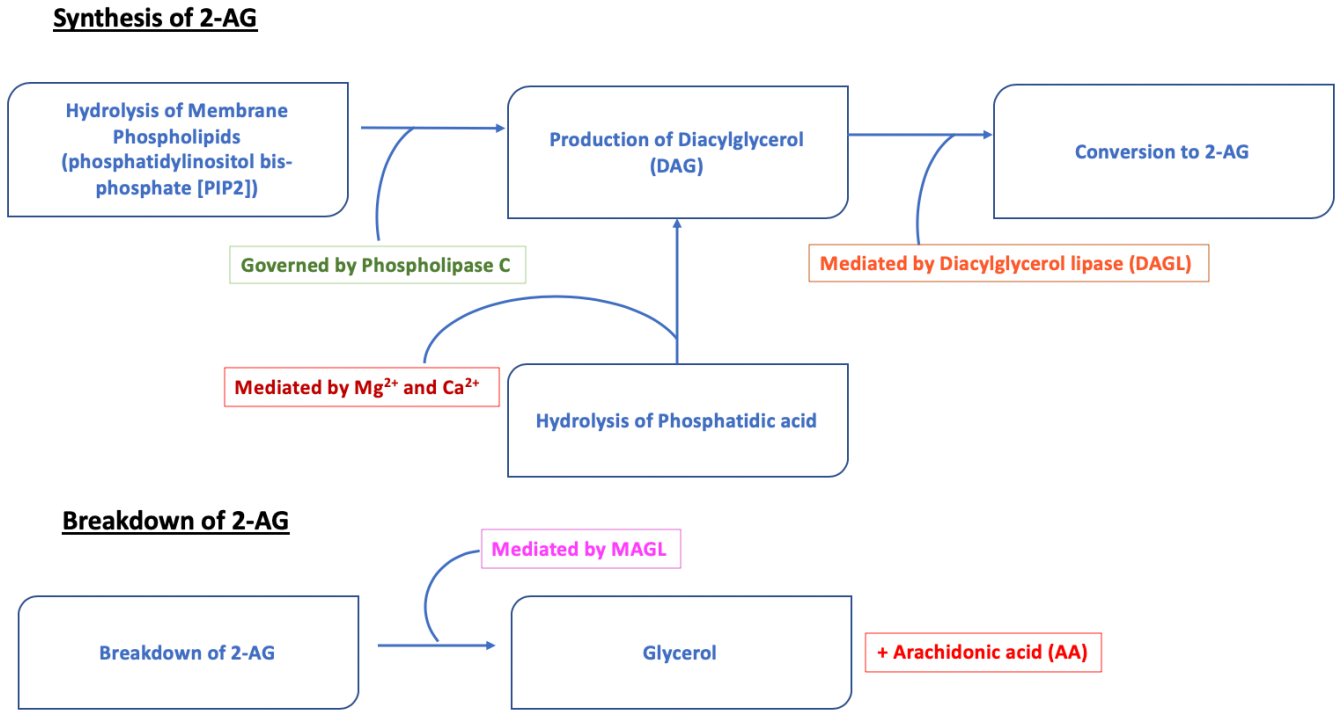

Figure 1.3: 2- AG can be synthesised by two pathways; First pathway involves the hydrolysis of the membrane phospholipid, phosphatidylinositol bis-phosphate (PIP2) which produced Diacylglycerol (DAG). This reaction is governed by Phospholipase C. DAG then converted to 2-AG by the activity of Diacylglycerol lipase (DAGL). Second pathway involves the hydrolysis of phosphatidic acid, which is mediated by the phosphohydrolase activity of the ions Mg^{2+} and Ca^{2+}, this in turn leads to the production of DAG. After this step, the remaining synthesis process of 2-AG is the same as the first pathway. 2-AG is degraded mostly by monoacylglycerol lipase and causes the production of glycerol and arachidonic acid as end products of this process.

The breakdown of 2-AG is initiated by the reuptake of a membrane transport molecule named AMT (AEA membrane transporter) (Maccarrone et al., 1998; Beltramo and Piomelli, 2000), and just like AEA, the signalling functionality of 2-AG is halted by this process

(Basavarajappa, 2007a; Ahn et al., 2008). Following this, the degradation of 2-AG occurs by monoacylglycerol lipase (MAGL) (Konrad et al., 1994) (Figure 1.3). MAGL was isolated and purified in adipose tissue, where it is found to be the catalyst for the ultimate step of triglyceride metabolism (Karlsson et al., 1997). Dinh et al. (2002) found that in rat cortical neurones the over-expression of MAGL led to the reduction in 2-AG levels. Furthermore, it was found by Dinh et al. (2004) that in MAGL knock out HeLa cells and rat brain fractions, the reduction in the hydrolysis of 2-AG was observed. Both of these studies established a direct correlation between the activity of both 2-AG and MAGL and how one impacts on the other. 2-AG is also metabolised through COX-2 into prostaglandin H_2 (PGH_2) (Sang et al., 2006) as well as FAAH (Simpson et al., 1991).

1.4 Endocannabinoid receptors and cannabinoid interactions

The ECS is comprised of several receptors, however only a few have been classified to date, these include CB1, CB2 and TRPV1 (McPartland and Pruitt, 2002). CB1 and CB2 belong to the superfamily of G-protein coupled receptors (GPCRs), that are made up of extracellular N-terminal and intracellular C-terminal tail, seven transmembrane domains that are linked via three intracellular loops (Basavarajappa, 2007b). TRPV belongs to the superfamily of Transient receptor potential proteins that are known to form gated cation channels triggered by multiple variables such as light, pressure, temperature and osmotic stress (Baylie and Brayden, 2010).

1.4.1. CB1

CB1 is a G-protein coupled receptor and the most abundant endocannabinoid receptor in the Central Nervous System (CNS) hence, it is also known as the 'brain cannabinoid receptor' (Iannotti et al., 2016). Also known as a metabotropic receptor (Aizpurua-Olaizola et al., 2017), it is found at high volumes in the brain regions such as the cerebellum, neocortex, basal ganglia, brain stem and hippocampus, amygdala and hypothalamus (Lu and Mackie, 2016; Kendall and Yudowski, 2017). It is found in decreased amounts in peripheral tissues, in regions such as vascular endothelium, eyes leucocytes, skeletal muscles, lungs, adrenal glands, spleen and testis (Howlett et al., 2002; Basavarajappa, 2007b; Kendall and Yudowski, 2017).

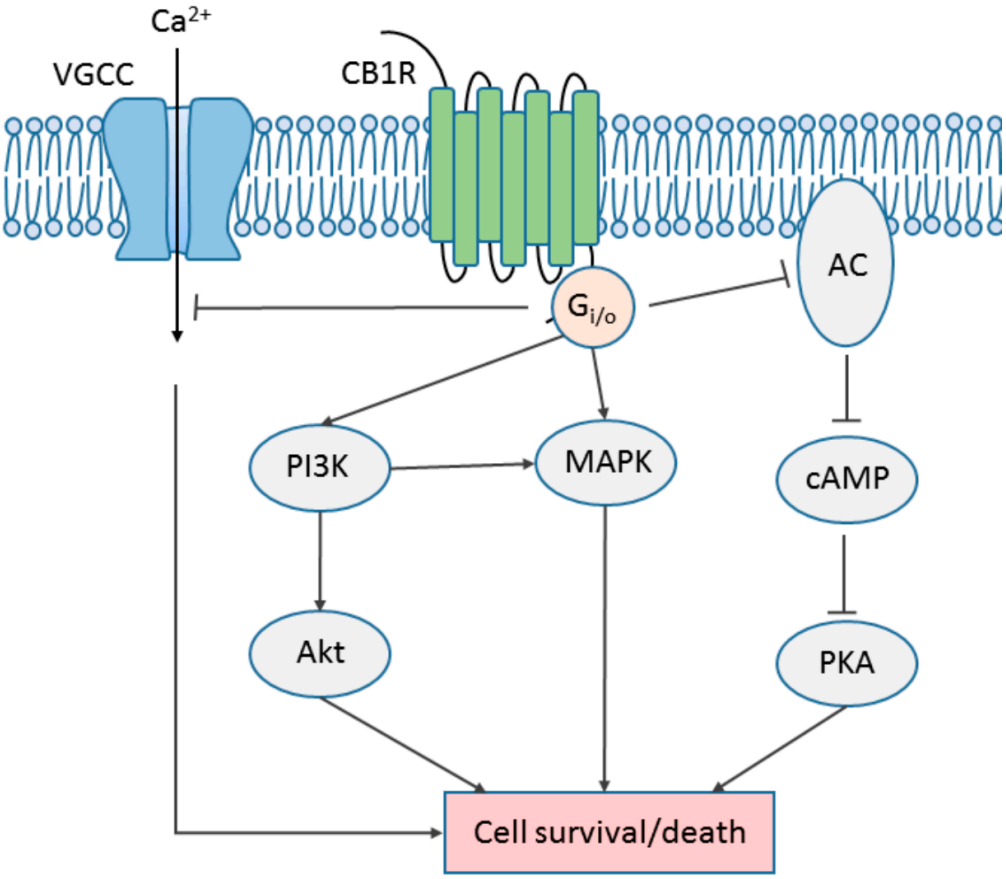

Figure 1.4 Some of the primary signalling pathways can be modulated by CB1 receptors (CB1R): 1) CB1 couples to the heterotrimeric G protein named Gi/o protein alpha subunit which suppresses adenylyl cyclase (AC) which in turn stops the production of cyclic adenosine monophosphate (cAMP) as well as halting the activity of protein kinase A (PKA). 2) CB1 can block the voltage-gated calcium channel (VGCC), further inhibiting calcium influx into the cells. 3) Mitogen- activated protein kinases (MAPK) can be stimulated by CB1 receptors, leading to elevated levels due to the decrease in adenylyl cyclase. 4) However, Adenylyl cyclase activity can be regulated by the activation of phosphoinositide 3-kinase (PI3K)/ protein kinase B (Akt) pathway. This therefore means that the increase in cell survival or cell death is dependent on the ligand and cellular environment in which the modulation of CB1 signalling occurs. Blunt arrows in the diagram represent inhibition and normal arrows represent stimulation by CB1 receptors. (Zou and Kumar, 2018).

The intracellular region of CB1 binds to the heterotrimeric G protein named Gi/o protein alpha subunit whose essential function is to halt the production of cyclic adenosine monophosphate (cAMP) from adenosine triphosphate (ATP) (Turu and Hunyady, 2009). Therefore, exogenous and endogenous ligands can cause an increased provocation of CB1 leading to downregulation of adenylate cyclase activity) (Figure 1.4). This results in a decrease of cAMP levels or elevates levels of mitogen-activated protein kinase (MAPK)

(Howlett, 1998; Turu and Hunyady, 2009) (Figure 1.4). Additionally, other categories of intracellular signals, e.g., phosphoinositide 3-kinase (PI3K) and protein kinase B (Akt/PKB) present in certain cell types, can be coupled to CB1 by Gi/o to regulate adenylyl cyclase (Gomez del Pulgar et al., 2000; Navarrete and Araque, 2010) (Figure 1.4). The vital functionality of the cAMP pathway is to regulate various cell activities which include cell proliferation, cell survival and cell distinction. Furthermore, this cAMP cascade is also responsible for controlling the function of several ion channels, such as; Voltage-gated Potassium (K+) and Calcium (Ca^{2+}) channels (Pertwee, 1997; Howlett and Mukhopadhyay, 2000; Sanchez, 2003; Witkowski et al., 2012). The activation of CB1 coupled Gi/o in neurons causes the inhibition of voltage activated Ca^{2+} channels (Iannotti et al., 2016).

1.4.2. CB2

CB2 receptors are more prevalent than CB1 in immune cells and tissues (Klein, 2005; Mackie, 2006). Their levels are much lower in the CNS in comparison to CB1 (Lu and Mackie, 2016). CB2 is mainly found in vascular elements (Ramirez et al., 2012), localized CNS macrophages (Mackie, 2008) and microglia (Walter et al., 2003). CB2 expression is also associated with nerve injury, inflammation and some pathological conditions (Van Sickle, 2005; Palazuelos et al., 2009; Viscomi et al., 2009). Research has indicated that the regulatory effects of CB2 receptors impact the microglial cells' functionality that plays a key role in the onset and progression of Alzheimer's disease as well as other basal ganglia associated disorders (Ramirez, 2005; Sagredo et al., 2007; Fernández-Ruiz et al., 2011).

1.4.3. TRPV1

TRPV1 differs from both CB1 and CB2 as it has six transmembrane domains, and consists of an extra intramembrane loop, which conjoins both the fifth and sixth transmembrane domains and shapes the pore channel region (Caterina et al., 1997; Iannotti et al., 2016). Various exogenous and endogenous agents such as some phytocannabinoids, AEA and N-oleyl-dopamine can activate these fundamental channels existing in TRPV1 (Van der Stelt et al., 2005; Marzo and Petrocellis, 2010; De Petrocellis and Di Marzo 2012; Iannotti et al., 2014), leading to an influx of calcium (Ca^{2+}) and sodium (Na^{+}) causing the depolarization of the cells inducing the physical/ neural effects of the stimuli which activated the receptor

(Liedtke et al, 2010). TRPV plays a key part in vasculature and can be sub divided into 6 sub-families, TRPV 1-4 (Baylie and Brayden, 2010).

1.4.4 Other receptors

Research has indicated that cannabinoids can interact with alternative receptors/targets. A study conducted by Bergamaschi et al. (2011) showed that elevated levels of CBD activated the hydroxytryptamine serotonin receptors (5-HT1A) which are responsible for various biological and neurological processes such as sleep, pain, perception, appetite and anxiety (Toth, 2003; De Matos Feijó et al., 2011; Leopoldo et al., 2011; Stiedl et al., 2015). Furthermore, cannabinoids can activate nuclear hormone receptors, specifically peroxisome proliferator activated receptors (PPAR) α, β and γ. Phytocannabinoids such as CBD (O'Sullivan et al., 2009; Granja et al., 2012), THC (O'Sullivan et al., 2005; Granja et al., 2012), cannabigerol (Granja et al., 2012) and cannabichrome (Granja et al., 2012) bind PPAR γ leading to either an increase in its transcriptional activity or influence its effects on selective antagonists. The endocannabinoids *N*- Oleoylethanolamine (OEA) (Fu et al., 2003; Sun et al., 2007; Hind et al., 2015) and Palmitoylethanolamide (PEA) (LoVerme et al., 2005; Borrelli et al., 2014) activate PPAR α altering its effects on selective antagonists. Some research has also shown that AEA and 2AG can activate PPAR α (Kozak et al., 2002; Sun et al., 2007; Romano and Lograno, 2012) and PPAR γ (Kozak et al., 2002; Ahn et al., 2015).

CBD has been shown to interact with G protein-coupled receptor 55 (GPR55), also known as an orphan G protein-coupled receptor (Bih et al., 2015). Research has implied that this could be due to the transmembrane domains (TD) framework of TD1, 2 and 3, since they resemble to those existing in CB1 and CB2 receptors (Whyte et al., 2009; Bih et al., 2015), thus suggesting a potential binding site for the cannabinoids on GPR55 (Baker et al., 2006; Whyte et al., 2009). This receptor is a ligand of lysophosphatidylinositol, and when activated it is responsible for the release of Ca2+ from intracellular stores which modulates hippocampal neurotransmission (Sylantyev et al., 2013). The binding of CBD to GPR55 has displayed antagonistic effects and help to support evidence of CBD being an anti-epileptic agent (Bih et al., 2015).

Lastly, reports by Leweke et al. (2012) and Seeman (2016) have suggested that CBD may be a partial agonist for dopamine D2 receptors, although more evidence is required to corroborate this.

1.5 Single celled protists and cannabinoids

1.5.1. Introduction to protists

Protists are eukaryotic, unicellular organisms that are either free-living, parasitic or endosymbionts (reviewed in Corliss, 2002). The free-living protists are ubiquitous and are abundant in soil, marine and freshwater environments (Foissner et al., 2008). For simplicity, protists can be broadly grouped into amoebae, ciliates and flagellates, based on their motility (Whittaker and Margulis, 1978; Adl et al., 2007). Of the three groups, ciliates are the most diverse, consisting of over 3500 identified species (Lanzoni et al., 2016). Ciliates are also considered the most evolved, as they possess a rudimentary mouth (Cytostome), a rudimentary anus (Cytoproct) and can reproduce sexually via conjugation (Foissner, 2008). They contain at least one macronucleus, which is essential for the ciliate's development processes (Brenner et al., 2001), together with one to several micronuclei, required for sexual reproduction; a process which flagellates, and amoebae cannot perform (Brenner et al., 2001).

Most ciliates are phagocytic heterotrophs, while mixotrophic species are found in a lower abundance (Mitra et al., 2016). Their cilia, along with motility, assist the ciliate with feeding; they guide the prey into the oral groove where the prey enter the cytostome (mouth) before being deposited into food vacuoles (phagosomes) (Adl et al., 2007; Lanzoni et al., 2016). Ciliates also possess a cytoproct (anus) for the exocytosis of undigested matter (Allen and Wolf, 1974). They primarily feed on bacteria, algae and other protists, with high ingestion rates (Fenchel, 1987) and as such, make a significant contribution to the microbial food chain whereby they are central to the transfer of energy, through organic compounds, between several trophic levels in the food web (Kathol et al., 2009; Xu et al., 2014). Ciliates also release inorganic compounds into the environment, via remineralisation, which include ammonia and phosphorus; key nutrients for their prey (Caron and Goldman, 1990).

1.5.2. Presence of ECS components in ciliates

Some research has examined whether the elements of the human endocannabinoid system are present and functional in protists, with the main test organism being the ciliate *Tetrahymena*.

1.5.2.1. Endocannabinoids

Anagnostopoulos et al. (2010) showed that *Tetrahymena thermophila* possesses a suite of endocannabinoids including NAEs, 2-AcGs and Free fatty acids (FFAs). The 6 main NAEs, in order of abundance, are N-γ-linolenoylethanolamine (GLEA), N-eicosenoylethanolamine (EEA), N-linoleoylethanolamine (LEA), N-palmitoylethanolamine (PEA), N-oleoylethanolamine (OEA) and N-stearoylethanolamine (SEA). A few other NAEs, including AEA, were also identified, but these were present at a very low concentration (Anagnostopoulos et al., 2010). GLEA is not common in nature, and SEA and EEA are present at very low concentrations in humans (Anagnostopoulos et al., 2010; Gaitán et al., 2018). LEA, OEA and PEA are more common in humans (Artmann et al., 2008) and activate similar receptors, mainly PPARs (α and γ) and TRPV1 (Kleberg et al., 2014).

1.5.2.2. Enzymes

The two main degrading enzymes, but not the synthesizing enzymes, of the endocannabinoid system have been reported to exist in *Tetrahymena*. Karava et al. (2001) was the first to show that *Tetrahymena pyriformis* possessed a functional FAAH enzyme, which could hydrolyse AEA and excrete a breakdown product amidohydrolase into the surrounding medium. The optimum pH for the enzyme was pH 9-10, which is similar to FAAH activity reported in variety of mammalian tissues and cell types (Karava et al., 2001). Moreover, Karava et al. (2005) showed that *T. thermophila* possesses 2 isoforms of FAAH: 46 and 66 kDa. The 66 kDa isoform is close in size of human and mammalian FAAH (63 or 67 kDa) (Giang and Cravatt, 1997; Maccarrone et al., 1998) while the 45 kDa is close to the 46 kDa FAAH in invertebrates (Matias et al., 2001). Anagnostopoulos et al. (2010) showed that the FAAH in *T. thermophila* could hydrolyse all of its endogenous NEAs, with the highest enzyme activity being evident with AEA.

Using Blast and phylogenetic tree comparisons, MAGL, which catalyses the breakdown of 2-AG was believed to be present in *T. thermophila* (McPartland et al., 2006). The presence of two isoforms (40kDa and 45kDa) was later confirmed experimentally by Evagorou et al. (2010). Two isoforms of MAGL have also been reported for several cell types (Bisogno et al., 1997; Dinh et al. 2002).

1.5.2.3. Receptors

McPartland et al. (2006) carried out a micro-genomic study to research the evolutionary transformation of the endocannabinoid system. The study involved investigating twelve phylogenetically varied organisms (including *T. thermophila*) and the functional orthologs (speciation related genes that have evolved to play the same biological role in different classes/species of organisms). The functional orthologs of receptors were limited to certain groups of organisms; TRPV1 and GPR55 (mammals), CB1- like receptors and DAGLα (animals), CB2 (Vertebrates). This study confirmed that none of the main endocannabinoid receptor genes (for CB1, CB2, TRPV1 and GPR55) were found in *T. thermophila.*

The above studies have indicated that *Tetrahymena* possesses a rudimentary ECS but to date, the receptor involved has not been identified. Even so, this ciliate can respond to exogenous cannabinoids (Section 1.5.3) but the target is currently unknown.

1.5.3. Effect of exogenous cannabinoids on protists

Only a handful of studies have tested the effects of cannabinoids on protists. McClean and Zimmerman (1976) showed a dose depended effect of Δ9-THC caused the cells of the ciliate *T. pyriformis* to become round and move in a sluggish manner; recovering after some hours (time not stated). Zimmerman et al. (1981) went on to show that *T. pyriformis* was most sensitive to Δ9-THC in the G2 phase of the cell cycle where the downregulation of both cAMP and cGMP led to an 8 to 15 minutes delay in the cell division.

Pringle et al. (1979) found that Δ9-THC did not affect motility of the amoeba-flagellate *Naegleria fowleri* but it did inhibit encystment and enflagellation, and reduced population growth in a dose-dependent manner. A reduction in amoeba population growth was also reported for *Acanthamoeba castellanii*, *Vermamoeba (Hartmannella) vermiformis*, and

Willaertia magna when treated with AEA, 2-O-acylglycerol (2-O-AG), and a non-hydrolyzable analogue of 2-O-AG, i.e. 2-O-AG ether (Dey et al., 2010). Population growth over three days was reduced by 58%, 96% and 68%, respectively, with all three compounds. The fact that 2-O-AG ether reduced population growth proved that it was the cannabinoid itself, and not any breakdown product that elicited the amoebic response (Dey et al., 2010).

In all these studies, the mode of action of cannabinoids has not been deduced. The cannabinoids appear to affect, in the main, population growth and considering this is reliant on successful feeding it is surprising that no study has yet evaluated the effect of cannabinoids on the feeding processes of *Tetrahymena*.

1.5.4. Ciliate feeding process

1.5.4.1. Ingestion

Pattern Recognition Receptors (PRRs) play a vital role in recognising non-self-ligands, i.e., bacterial motifs termed Pathogen-Associated Molecular Patterns (PAMPs) (reviewed in Janeway and Medzhitov, 2002), in phagotrophs/macrophages in innate immunity (Vogel et al., 1980; Pauwels et al., 2017). PRRs identified in protists to date have been members of the C-type lectin superfamily, which is enclosed of 17 subgroups of glycoproteins (Drickmer and Taylor 2015; Boskovic et al., 2006), and primarily involved in recognising carbohydrate ligands from bacterial LPS and fungal cell walls (Stahl and Ezekowitz, 1998; East and Isacke, 2002). Some carbohydrates recognised by C-type lectins are: Glucose, L-fucose, N-acetylgalactosamine (GalNac), N-acetylglucosamine (GlcNAc), galactose and mannose (Drickamer and Fadden., 2002). Due to the diverse nature of C-type lectins, they have found to be involved in various processes such as platelet activation, pathogen recognition, phagocytosis cell binding and cell differentiation (Ramoino et al., 2001; Cambi et al., 2005; Roberts et al., 2006; Gupta and Gupta., 2012; Al-hammadi., 2020). As well as this, this glycoprotein superfamily has been shown to influence prey capture processes in amoebae and can incur binding to carbohydrate ligands present on bacteria utilising an extracellular carbohydrate recognition domain (CDR) which is calcium dependent (Kerrigan and Brown., 2009, Alenton et al., 2017).

The mannose receptor has been shown to be involved in feeding in the amoebae *Entamoeba histolytica* (Bracha et al., 1982) and *Acanthamoeba castellanii* (Allen and Davidowicz, 1990; Alsam et al. 2005) and in the marine dinoflagellate *Oxyrrhis marina* (Wootton et al., 2007). The mannose receptor has also been implicated in the feeding of the ciliates *Euplotes mutabilis* (Wilks and Sleigh, 2004) and *T. pyriformis* (Dürichen et al., 2016). The Gal/GalNAc receptor has been shown to be involved in the feeding of the amoebae *E. histolytica* (Bär et al., 2015) and *V. vermiformis* (Venkataraman et al., 1997; Harb et al., 1998) but not in the dinoflagellate *O. marina* (Wootton et al., 2007). The Gal/GalNAc receptor has been also implicated in the feeding of the ciliates *Euplotes vannus* (Roberts et al., 2006) and *E. mutabilis* (Wilks and Sleigh, 2004).

Another group of glycoprotein surface membrane receptors are Scavenger receptors (SRs) which are divided into ten sub classes (A to J) (Zani et al., 2015). Class A and B SRs (SR-A, SR-B) have cysteine-rich domains similar to the C-type lectins and are the most commonly involved SRs in macrophage phagocytosis (Peruń et al., 2016). Both types can recognise bacterial cell structures such as lipoteichoic acids from Gram-positive bacteria (Dunne et al., 1994; Baranova et al., 2008) and lipid A from the LPS of Gram-negative bacteria (Hampton et al., 1991; Stuart et al., 2005). Recently, the scavenger receptors LmpA and LmpB were reported to be involved in prey uptake in *Dictyostelium discoideum.* LmpA was isolated in phagolysomes and endosomes and seemed to be involve in the phagocytosis of mainly Gram-positive bacteria, whereas LmpB was confined in the plasma membrane and early phagosomes and was solely involved in the uptake of Gram-positive prey (Sattler et al., 2018). It is unknown whether *Tetrahymena* possesses scavenger receptors.

When the ciliate ingests a bacterial prey, signalling pathways involving PRRs recognise this bacterial intake and activate the food processing mechanisms, i.e., formation of food vacuoles/phagosomes (Muller, 1980a,b; Wootton et al., 2007). These signalling pathways cause the restructuring of the actin cytoskeleton, leading to the generation of pseudopod-like structures that surround the prey and form the phagocytic cup (Pauwels et al., 2017). A contractile force driven by myosin helps seal the two ends of the pseudopods (Swanson, 2008) and recruitment of dynamin leads to the vacuole detaching from the surface and moving into the cytoplasm (Marie-Anaïs et al., 2016).

1.5.4.2. Digestion

Once the food vacuole is in the cytoplasm it goes through various stages of maturation (Levin et al., 2016). In the initial stage of the maturation process the phagosome undergoes fusion with early endosomes and acquires proteins such as GTPases and Ras related protein Rab5 (Rab5). The effector present in Rab5, called Rabaptin-5 obtains a class III phosphatidylinositol 3-Kinase vacuolar protein sorting 34 (PIK3 VPs34), which reacts with other molecules, entailing a cyclic collection of Phosphatidylinositol 3- phosphate (PIP3) in the phagosome (Vieira et al., 2001). PIP3 aids the attachment of early endosomal antigen 1 (EEA1) and class C core vacuole/endosome tether (CORVET) complex target membranes onto the phagosome membrane (Lawe et al., 2001; Peplowska et al., 2007). As well as this, v-ATPase is recruited, which triggers acidification within the phagosomal lumen, initiated by pumping of protons, leading to breakdown of the particles (Figure 1.5).

The maturation process involves the change of Rab5 to Ras related protein Rab7 early phagosome to late phagosome leading to the alteration of CORVET to homotypic fusion and vacuole sorting (HOPS) (Rink et al., 2005). Rab7 is fundamental for the maturation process as this initiates phagosome movement along with recruitment of Lysosomal-associated membrane protein 1 and 2 (LAMP1 and LAMP 2) (Harrison et al., 2003; Huynh et al., 2007). These proteins aid the phagosomes to fuse with acidic lysosome structures by allowing them to pass through the plasma membrane and conjoin with the food vacuole internally (Jacobson and Anderson, 1996; Pauwels et al., 2017). The resultant ‘phagolysosome’ can be arbitrated by various soluble NSF attachment protein receptors (SNAREs) (Luzio et al., 2000). This increases the degradation processes in the phagosome due to the acquisition of hydrolytic enzymes, e.g., lipases, DNAses, glycosidases and proteases and cathepsins which function optimally in a low pH acidic environment and causes the breakdown of the cargo (Yates et al., 2009). Reactive oxygen species (ROS) are produced by Nicotinamide adenine dinucleotide phosphate (NADPH) oxidases during the degradation process (Duclos, 2003; Savina et al., 2006; Luzio et al., 2010).

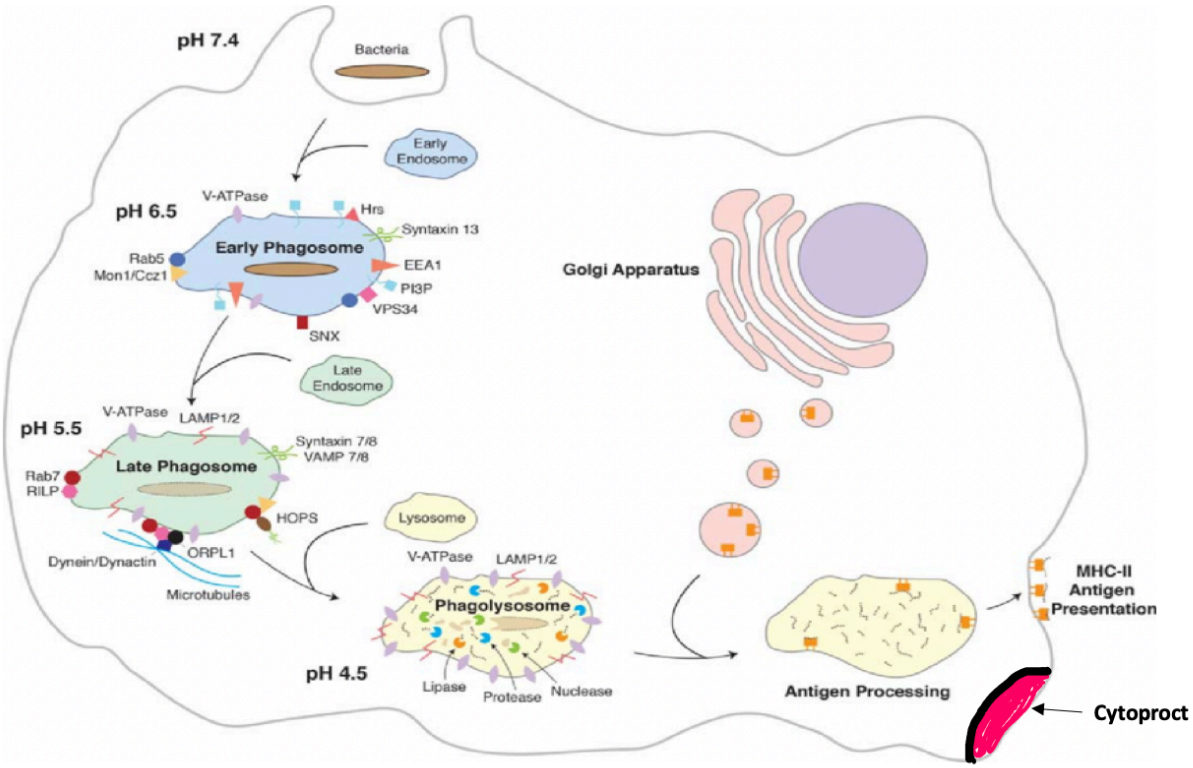

Figure 1.5: Different phases of phagosome maturation in a phagocyte. The process of Phagocytosis involves a sequence of fission and fusion events associated with the endocytic vesicles and phagosomes, leading to the acidification of the phagosomes, phagosomes and lysosomes integration which eventually causes the formation of phagolysosomes (Poirier and Av-gay, 2015). This process initiates by engulfment of micro-organisms by the phagocyte, into the phagosome (an organelle derived from the plasma membrane). After which the micro-organisms captured within the phagosome the react with the endosomal pathways: 1) Early phagosome fuses with early endosomes and acquires Ras-related protein Rab 5 and other proteins such as syntaxin 13 which is a soluble NSF attachment protein (SNARE)- required for vesicle trafficking (Prekeris et al., 1998) and Hrs (Hepatocyte growth factor regulated tyrosine- kinase substrate)- involved in late endosomal sorting (Vieira et al., 2004). 2) Rab 5 acquires class III phosphatidylinositol 3-kinase vacuolar protein sorting 34 (PIK3 VPS34), which in turn reacts with other molecules causing a cyclic collection of phosphatidyl 3- phosphate (PIP3) in the phagosome (Poirier and Av-gay, 2015). 3) Sorting nexin protein (SNX) is recruited to aid PIP3 in the attachment of early endosomal antigen 1 (EEA1) (Chua and Wong, 2013) and class C core vacuole/ endosome tether complex (CORVET) to the phagosome membrane (Lawe et al., 2001; Peplowska et al., 2007). 4) VTPASE is then recruited to establish proton pumping in the phagosome lumen leading to acidification of the phagosome and further entailing particle breakdown (Poirier and Av-gay, 2015). 5) Mon1-Ccz1 also known as the guanine nucleotide exchange factor (GEF) is recruited for the conversion of Rab 5 to Ras-related protein Rab 7 during the phagosome maturation process (Nordmann et al., 2010). 6) Rab 7 is vital for this process as it initiates the phagosome movement by associating with the Rab- interacting lysosomal protein (RILP), which therefore bridges the phagosome with dynein – dynactin (microtubule-associated motor complex) (Harrison et al., 2003). 7) Rab 7 recruits Lysosomal associated membrane-

protein (LAMP1/ 2) and Vesicle associate membrane proteins (VAMP7/ 8) which are important for the fusion of the phagosome and lysosome (Huynh et al., 2007; Vieira et al., 2002). 8) The change of the Rab proteins further causes the change to the early phagosome to a late phagosome and alters CORVET to homotypic fusion and vacuole sorting (HOPS (Rink et al., 2005). The oxysterol-binding protein homologue (ORPL1) is recruited by HOPS to localize late endosome with the late phagosome (Johansson et al., 2005). 9) The recruited proteins help to join the phagosome to the acidic lysosome by allowing the lysosome to pass through the plasma membrane and join the phagosome internally, making a phagolysosome complex. 10) Other SNARE proteins such as syntaxin 7/8 are recruited by the phagolysosome (Luzio et al., 2000) and help to increase the degradation processes within by further obtaining hydrolytic enzymes e.g. DNAses, lipases, proteases, nucleases etc (Yates et al., 2009). This overall leads to the breakdown of the cargo (micro-organism matter) within the phagolysosome (Poirier and Av-gay, 2015).

Allen and Fok (1980) showed that vacuole membrane availability in a ciliate cell is limited; therefore, the food vacuole membrane has to be recycled in order to be reused for the production of new food vacuoles. Indigestible phagosomal cargo diffuses out through the cell membrane and into the cytoproct of the ciliate where it is expelled via the process of exocytosis (Allen and Wolf, 1974; Satir, 1989). The retromer complex proteins, Rab4, Rab10 and Rab11 are then responsible for recycling other phagosomal cargo proteins back to the plasma membrane or trans- Golgi network to allow for new food vacuole formation (Damiani et al., 2004; Wollert and Hurley, 2010).

Food vacuoles therefore have a definitive ‘life-span’ in a cell, known as the Vacuole Passage time (VPT) which includes the processes of ingestion, food vacuole formation and exocytosis (Allen and Fok, 1980; Capriulo and Degnan 1991). Thurman et al. (2010) reported that the minimum VPT in *T. pyriformis* was *ca*. 30 min but because the ciliate has only one cytoproct, and vacuoles need to queue inside the cell (in the order they were formed) before being exocytosed, some vacuoles are present in the cell for longer. Other studies have also suggested that the first vacuoles formed are the first to be defecated in *T. pyriformis* (Rothstein, 1974; Ricketts and Rappitt, 1976; Ricketts, 1979; Ricketts, 1983).

1.6 Rationale and overall aim of this study

The endocannabinoid system has been investigated as a potential target for the pharmacotherapeutic treatment of various diseases. However, many of the effects cannot be attributed exclusively to the activation of the more common cannabinoid receptors (e.g.

CB1 and CB2) and studies suggest cannabinoids can interact with a variety of other molecular targets (Bih et al., 2015). The use of a ciliate model to elucidate these 'other' targets is attractive because they do not possess any of the common receptors yet respond to exogenous cannabinoids. The overall objective of this study was therefore to examine the effect of exogenous CBD and AEA on prey ingestion and food vacuole formation in the ciliate *T. pyriformis* and deduce which stage of the feeding process was being affected by these cannabinoids.

2. Methods and Materials

2.1. Organisms and maintenance

2.1.1. Preparation and maintenance of prey

The heterotrophic bacterium *Klebsiella aerogenes* (National Collection of Type Culture [NCTC] 9528) was grown as streak plates on Lysogeny Broth (LB) Agar plates (Appendix 1) and incubated at 25°C for 48 h. A concentrated cell suspension was made by pouring *ca*. 10ml of sterile water onto two plates and dislodging the cells with a sterile spreader. This suspension was stored at 4°C and used to routinely feed the ciliate *Tetrahymena pyriformis* (see 2.1.2).

The autotrophic bacterium *Synechococcus* sp. KH-3 (Dillon & Parry, 2008) was used as the main prey in experiments. It was grown in Blue Green 11 (BG 11) broth (Appendix 1) on a rotary shaker at 23°C, 7 days prior to experiments. Following this, 10ml sub-samples were centrifuged at 3500 rpm for 10 min and then 9ml of the supernatant was removed. The remaining 1ml samples were pooled to give a concentrated stock suspension.

A suspension of 0.49µm diameter fluorescently-labelled yellow/green microspheres ('beads') (Fluoresbrite™ Polyscience Inc.), of known particle concentration, was stored at 4°C. The suspension was sonicated for 5 min prior to experiments.

2.1.2. Preparation and maintenance of *Tetrahymena pyriformis*

T. pyriformis was grown in 400ml Chalkley's medium (Appendix 1) supplemented with *ca*. 2ml of *K. aerogenes* suspension (2.1.1), at room temperature (23°C), 3 days prior to each experiment. Sixteen 15ml samples were centrifuged at 2000rpm for 15 min and then 14ml of the supernatant was removed. The remaining 1ml samples were pooled to give a concentrated stock suspension. Pulse-chase experiments (Section 2.6) required a ciliate suspension at a higher concentration, so more than 16 sub-samples were centrifuged and pooled, then re-centrifuged to concentrate cells further. This gave ciliate starting concentrations of at least 8×10^4 cells/ml.

2.2. Counting cells

2.2.1. Counting *T. pyriformis*

An aliquot (normally 100µl) of *T. pyriformis* suspension was fixed with glutaraldehyde (0.5% v/v final conc.), i.e., 5µl of 10% (v/v) glutaraldehyde was added to 100µl sample. The sample was loaded into 2 haemocytometers, each with 2 counting grids and viewed with a light microscope (x40 magnification). Each counting grid comprised 9 medium-sized squares and the number of cells in each was determined (36 squares in total). The average number of cells per square was multiplied by 10^4 to give cells/ml.

2.2.2. Counting *Synechococcus* sp.

Serial dilutions of the *Synechococcus* suspension were prepared down to 10^{-3}. A 200µl sample was taken from either the 10^{-2} or 10^{-3} and filtered onto a 0.2µm pore-sized filter (Millipore) with the aid of a suction pump. The filter was placed onto a slide, on top of some immersion oil, and a drop of oil placed on top of the filter followed by a cover slip. A further drop of oil was placed onto the coverslip before viewing the slide with an epifluorescence microscope. Since the cells contain chlorophyll a, they fluoresce red under green excitation. The number of cells in randomly chosen Whipple Grids (housed in an eye-piece) was determined until at least 400 cells had been counted. The average number of cells/Whipple grid was multiplied by 23068 (to determine the number of cells on the filter) and knowing what volume and dilution of suspension had been used, the cell concentration (cells/ml) in the undiluted suspension was determined.

2.2.3. Counting *Synechococcus* and beads inside ciliate cells

Samples from experiments were fixed with glutaraldehyde (0.5% v/v final conc.) and 8µl applied to a slide, followed by a coverslip and drop of immersion oil. In pulse-chase experiments, ciliate concentration after the chase was too low to observe enough ciliates using this method so 1ml of fixed sample was filtered onto a 1.2µm pore-sized filter (Millipore) and mounted onto a slide as described in 2.2.2. The number of *Synechococcus* cells or beads, and the number of food vacuoles, in ten *T. pyriformis* cells were counted per replica sample to provide data on prey/cell (P/C), vacuoles/cell (V/C) and prey/vacuole (P/C

divided by V/C). *Synechococcus* cells and fluorescent beads were counted under green and blue excitation, respectively.

2.3. Cannabinoids and PPARα receptor agonist and blockers

Cannabidiol (CBD) and Anandamide (AEA) (TOCRIS) were maintained as 10mM and 14.4mM stock solutions, in ethanol, respectively. They were stored at -20^{o}C. The standard concentration used in experiments was 4µM (close to their IC50 values, Jones 2017): for an experimental tube containing 1ml of *T. pyriformis*, 40µl of 10^{-2} dilution of CBD or 28µl of 10^{-2} dilution of AEA was used.

The PPARα agonist, Oleoylethanolamine (OEA) (TOCRIS), and PPARα blocker, GW6471 (TOCRIS), were both maintained as 10mM stock solutions, in ethanol, at -20^{o}C.

2.4. Effect of cannabinoids on *Synechococcus* sp.

Synechococcus sp. was incubated with CBD and AEA (each at 4 and 8µM), in triplicate, for 180 min. Cell concentration was determined at T_{zero} and T_{180h} (see 2.2.2) and compared against the control (no AEA/CBD) to determine whether the bacterium was directly affected by the cannabinoids (*it was not*).

2.5. Feeding Experiments

2.5.1. Basic experimental procedure

Experimental tubes contained 1ml *T. pyriformis* (variable concentration) and $1x10^{7}$ cells/ml of *Synechococcus*. The 'test' tubes contained either CBD or AEA (normally 4µM) whilst the 'control' tubes did not (all in triplicate). Experiments were performed at 23^{o}C and samples were removed throughout the experiment, fixed with glutaraldehyde and the P/C, V/C and P/V determined for each replicate (see 2.2.3) and then averaged. Each of the three parameters (±Standard Error of the Mean [SEM]) were plotted against time.

To determine ciliate ingestion rate (prey/cell/min), linear regression analysis was performed on the initial linear portion of P/C vs time, for each of the triplicates. Any lag phase in

feeding (min) was determined from these linear regressions – where the line crossed the horizontal axis (P/C = zero). All data were then averaged (±SEM).

2.5.2. The effect of AEA and CBD on prey ingestion by *T. pyriformis*

Two 180 min experiments were performed to monitor the effect of AEA and CBD (both at 4µM) on *T. pyriformis* feeding. Samples were removed every 2 min (until 30 min) and then every 5 min (from 35 min to 180 min) for the control. For the samples containing CBD and AEA samples were removed every 10 min (until 30 min) and then every 5 min (from 35 min to 180 min). Samples were fixed and processed as described in 2.5.1.

2.5.3 Involvement of *Synechococcus* in feeding lag phase induced by cannabinoids

In 2.5.2, both AEA and CBD induced a lag phase prior to feeding (see 3.3). To deduce whether this might be an indirect effect, due to absorption of cannabinoids into *Synechococcus* cells and subsequent effect on ciliate after ingestion, a 45 min experiment was performed. *Synechococcus* was pre-incubated with 4µM AEA or CBD for 1 h then washed 6 times (1 wash = centrifugation at 3500rpm for 10 min and replacement of supernatant with Chalkley's medium followed by vortexing). Treated and untreated *Synechococcus* were fed to *T. pyriformis* and samples taken every 2 min (until 30 min) and then every 5 minutes (35 min to 45 min). Samples were fixed and processed as described in 2.5.1.

2.5.4 Effect of using a non-living prey on lag phase induced by cannabinoids

To further prove that the cannabinoids were having a direct (and not an indirect) effect on the ciliate, a 180 min experiment was performed with fluorescent beads (Inert prey) following 2.5.2.

2.5.5 The effect of AEA and CBD on vacuole trafficking and defecation by *T. pyriformis*

This pulse-chase experiment was performed once and involved the monitoring of *Synechococcus*-containing food vacuoles in *T. pyriformis* over a 120 min period, with and without a 'chase' step (with/without CBD/AEA) at 15 min.

Controls: Three tubes contained *T. pyriformis* and $1x10^7$ *Synechococcus* cells/ml only, were sampled every 5 mins from 0-120mins to determine V/C ('**Control – un-chased**' x3). At 15 min, 0.5ml sub-samples from each tube was added to 24.5ml Chalkleys (a 1 in 50 dilution – the 'chase') and these were also sampled every 5 mins to 118 mins ('**Control – chased**' x3). This dilution aimed to reduce the *Synechococcus* prey concentration to such a level that it was no longer possible for the ciliate to consume it (or produce new fluorescent vacuoles), and allow the evaluation of the persistence of *pre-existing vacuoles only* from 15 to 118 mins. To confirm that the dilution did stop feeding, three tubes containing *T. pyriformis* and *Synechococcus* at $2x10^5$ cells/ml ('**Residual uptake**' x3), were included and sampled every 5 mins to 120 mins to determine V/C.

Tests: For each test (+CBD, +AEA), three tubes containing *T. pyriformis* and $1x10^7$ *Synechococcus* cells/ml only were sampled every 5 mins from 0-15 mins. Then, a 0.5ml sub-sample from each tube was added to 24.5ml Chalkleys + cannabinoid (at 4µM) and subsequently sampled every 5 mins to 118 mins ('**Test – chased**' x3). Immediately after this, the cannabinoid was also added to the undiluted tubes (at 4µM) and sampled every 5 mins to 120 mins ('**Test – un-chased**' x3).

All sub samples (100µl pre-chase, 1ml post-chase) were fixed with glutaraldehyde (0.5% final conc.) and V/C determined (see 2.2.3). Data post-chase were corrected for any residual formation of vacuoles. Rates of vacuole formation/loss were determined with linear regression analysis on each of the triplicates and then averaged (±SEM).

2.5.6 Effect of cannabinoid concentration on lag phase and feeding rates

Ninety-minute feeding experiments were performed with a range of CBD and AEA concentrations: 0 µM, 0.25µM, 0.5µM, 0.75µM, 1µM, 1.25µM, 1.5µM, 1.75µM, 2µM, 2.25µM, 2.5µM, 2.75µM, 3 µM, 3.25µM, 3.5µM, 4 µM and 4.5µM. Samples were removed every 2 min (until 30 min) and then every 5 min until (90 min) for the control and every 5 min (until 90 min) for both AEA and CBD. Samples were processed as described in 2.5.1 with prey/cell being determined up until at least two complete food vacuoles had been formed in the cell. Graphs were plotted of ingestion rate and lag phase duration against cannabinoid concentration.

2.5.7 Evaluating whether the molecular target for CBD is PPARα

Wanlahbeh (2020) showed that blocking PPARα with the antagonist GW6471 completely alleviated CBD-induced cell death in *T. pyriformis*. Its effect on feeding was tested in a ninety-minute feeding experiment whereby *T. pyriformis* was treated with (i) CBD alone (4µM), (ii) the PPARα blocker GW6471 alone (10µM), (iii) CBD (4µM) with GW6471 (10µM) and (iv) no CBD or blocker (Control). Considering OEA is a natural ligand for PPARα, an additional experiment was performed alongside this with tubes containing, (i) OEA alone (45µM – its IC50 for *T. pyriformis* [Wanlahbeh, 2020]), (ii) GW6471 alone (90µM) and (iii) OEA (45µM) with GW6471 (90µM). Samples were taken over 90 min and processed as described in 2.5.1.

2.6 Statistical analysis

Data for two variables were statistically compared using an independent student t test. Data for more than two variables were compared using a one-way ANOVA, followed by a post-hoc Tukey test. Both used a confidence limit of 95% ($P \leq 0.05$).

3. Results

3.1. Effect of CBD and AEA on *Synechococcus* survival

Synechococcus sp. was incubated with CBD and AEA (each at 4 and 8µM), and no cannabinoid (Control), for 180 min and cell concentration determined at T_{zero} and T_{180h} (Table 3.1). There was no significant effect of either cannabinoid, at either concentration, on cell survival (ANOVA, P>0.05).

Table 3.1: *Synechococcus* concentration (cells/ml) at T_{zero} and after incubation for 180 min (T_{180}) with AEA or CBD (4 and 8µM) or no cannabinoid (Control). n=3.

Treatment	Cells/ml (±SEM)	
	T_{zero}	T_{180}
Control	$1.17\pm0.31\times10^8$	$1.05\pm0.43\times10^8$
CBD (4µM)	$0.96\pm0.16\times10^8$	$1.00\pm0.44\times10^8$
CBD (8µM)	$1.11\pm0.11\times10^8$	$1.08\pm0.24\times10^8$
AEA (4µM)	$0.98\pm0.52\times10^8$	$1.02\pm0.50\times10^8$
AEA (8µM)	$1.06\pm0.15\times10^8$	$1.13\pm0.10\times10^8$

3.2. Effect of 'pre-loading' *Synechococcus* with CBD and AEA on *T. pyriformis* feeding

Synechococcus was pre-incubated with 4µM AEA or CBD for 1 h then washed 6 times before feeding the cells to *T. pyriformis*. Untreated *Synechococcus* (Control) was also fed to the ciliate. There was no effect of feeding 'pre-loaded' *Synechococcus* to the ciliate (Figure 3.1) suggesting that if AEA/CBD showed a negative effect on the ciliate in later experiments, it would be due to a direct response on the ciliate cell itself and not an indirect response of ingesting an affected prey.

3.3. Effect of CBD and AEA (4µM) on *T. pyriformis* feeding on *Synechococcus*

Experiments were performed to examine the effect of AEA and CBD (both at 4µM) on *T. pyriformis* feeding on *Synechococcus* over a 3h period. Data for prey/cell and vacuoles/cell over time are shown in Figure 3.2 (data for prey/vacuole in Appendix 2).

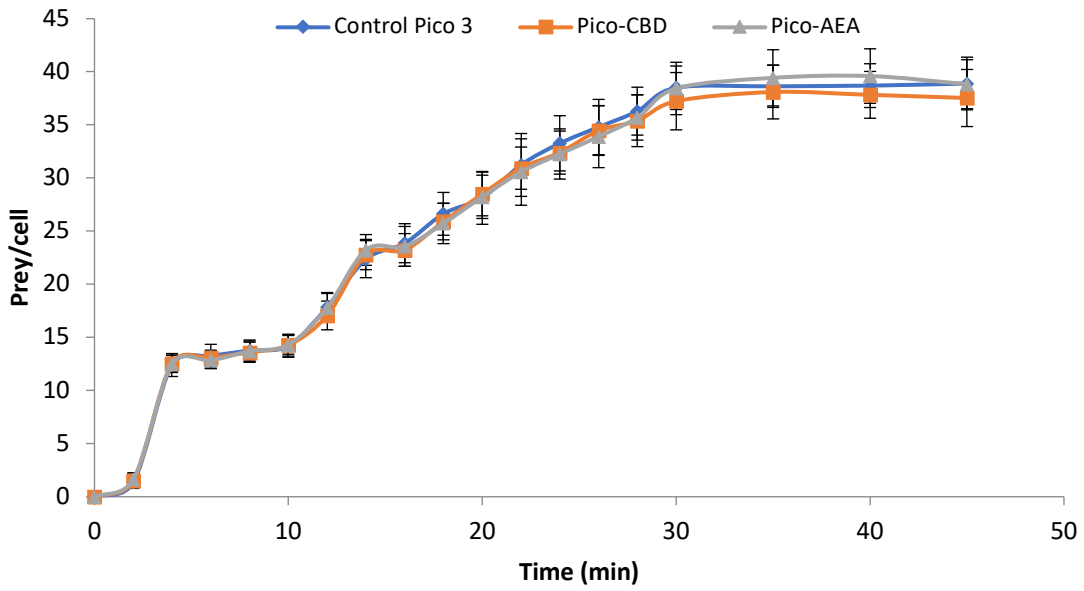

Figure 3.1: *T. pyriformis* was fed with *Synechococcus* ('Pico') at 1x10^7 cells/ml and the average number (±SEM) of prey per ciliate cell was determined over 45 min. Pico-CBD and Pico-AEA had been pre-incubated with 4µM CBD or AEA, respectively while Control-Pico had not been pre-incubated with either cannabinoid. Error bars are SEM. n=3.

The untreated ciliate (Control) showed no lag period before feeding commenced (Figure 3.2). Two phases of feeding were then recorded, before reaching satiation at *ca*. 150 min. There was an initial phase of feeding (Phase 1: 0-30 mins), followed by no feeding (30-50 min), followed by a second phase of feeding (Phase 2: from 50 min) (Figure 3.2). The ingestion rate (IR) and vacuole formation rate (VFR) in the second phase were significantly lower (T-Test, P<0.01), being 60% and 33% the rate in phase 1, respectively (Table 3.2). In the presence of AEA, the ciliate exhibited a lag of 31.28±0.37 min (based on prey/cell) and 29.89±0.80 min (based on vacuoles/cell) (Table 3.2); these were not significantly different to each other (T-Test, P=0.15). Following this, feeding proceeded in two phases. The IR and VFR in Phase 1 (30 to 50 min) were not significantly different to the rates exhibited by the Control in its Phase 1 (Table 3.2). Then, in Phase 2 (from 50 min) the IR and VFR were, (i) significantly lower (P<0.01) than the Phase 1 rates (IR at 83% and VFR at 47%) and, (ii) significantly higher than the rates exhibited by the Control in its Phase 2 (Table 3.2). At satiation, the AEA-treated cells contained the same number of prey as the Control, but the number of vacuoles and number of prey within those vacuoles was significantly higher (Table 3.2).

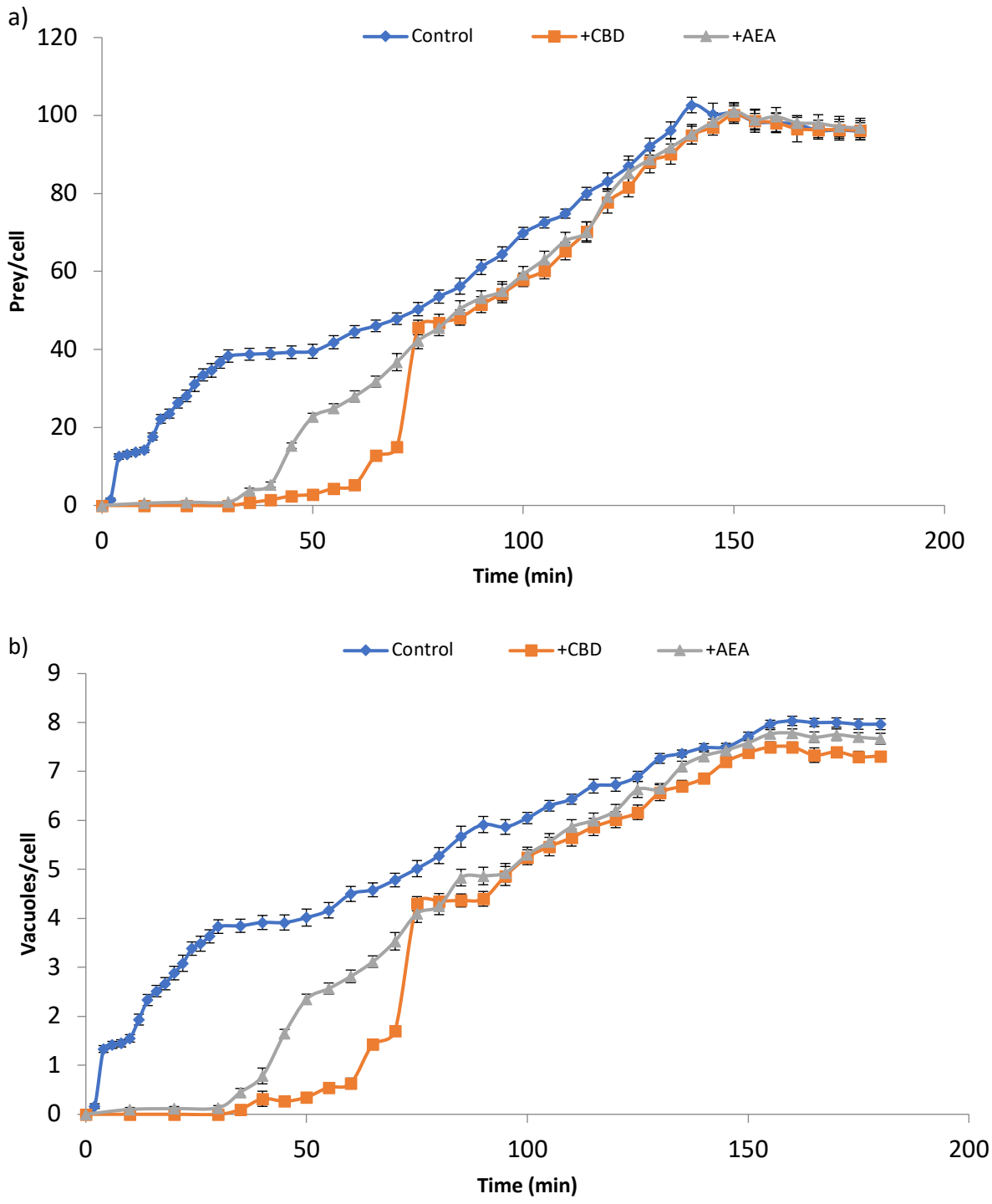

Figure 3.2: *T. pyriformis* was fed with *Synechococcus* at 1x10^7 cells/ml in the absence (Control) or presence of CBD and AEA (4µM). The average number (±SEM) of a) prey per ciliate cell and b) vacuoles per ciliate cell was determined over 180 min. n=6.

Table 3.2: Feeding parameters (average±SEM) when *T. pyriformis* feeds on *Synechococcus* ($1x10^7$ cells/ml) in the absence (Control) and presence of 4µM CBD (+CBD) or AEA (+AEA). Significantly different to control at P<0.05* or P<0.01** (Tukey's HSD). CBD significantly different to AEA at P<0.05^ or P<0.01^^ (Tukey's HSD). n=6.

Parameter	**Control**	**+CBD**	**+AEA**
Phase 1 of feeding			
Lag phase (based on prey/cell)	0.00±0.00	59.13±0.27**^^	31.28±0.38**
Lag phase (based on vacuoles/cell)	0.00±0.00	57.82±0.45**^^	29.89±0.80**
Ingestion rate, IR (prey/cell/min)	1.23±0.05	2.32±0.13**^^	1.00±0.09
Vacuole formation rate, VFR (vacuoles/cell/min)	0.12±0.01	0.21±0.01**^^	0.11±0.00
Phase 2 of feeding			
Ingestion rate, IR (prey/cell/min)	0.74±0.03	0.91±0.02**^	0.83±0.02*
Vacuole formation rate, VFR (vacuoles/cell/min)	0.04±0.00	0.05±0.00**^^	0.05±0.00**
At satiation (150-180min)			
Prey/cell	98.48±0.77	97.17±0.53	98.13±0.57
Vacuoles/cell	7.99±0.05	7.40±0.05**^^	7.73±0.05**
Prey/vacuole	12.15±0.11	13.02±0.11**	12.68±0.11**

In the presence of CBD, the ciliate exhibited a lag of 59.13±0.27 min (based on P/C) and 57.82±0.45 min (based on V/C) (Table 3.2); these were significantly different to each other (T-Test, P=0.03). Following this, feeding proceeded in two phases. The IR and VFR in Phase 1 (60 to 75 min) were significantly higher than the rates exhibited by the Control and AEA-treated cells in Phase 1; being twice as high (Table 3.2). Then, in Phase 2 (from 75 min) the IR and VFR were, (i) significantly lower (T-Test, P<0.01) than the Phase 1 rates (IR at 39% and VFR at 22%) and, (ii) significantly higher than the rates exhibited by the Control and AEA-treated cells in their Phase 2 (Table 3.2). At satiation, the CBD-treated cells contained the same number of prey as the Control and AEA-treated cells but they contained significantly fewer vacuoles containing significantly more prey (Table 3.2).

To further confirm that AEA and CBD were directly affecting the ciliate cells, one of these 3h experiments included fluorescent beads as the prey (Figure 3.3). The patterns of cannabinoid effects were the same as those obtained with *Synechococcus*, and no significant difference in calculation IR and lag phases was recorded (Table 3.3).

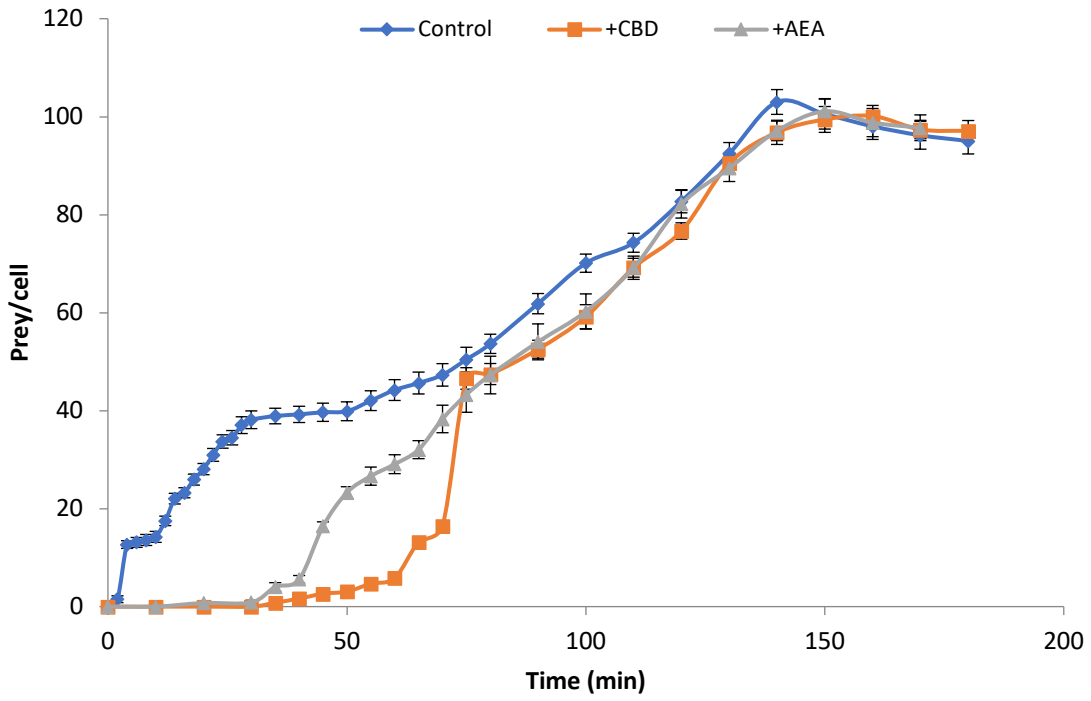

Figure 3.3: *T. pyriformis* was fed with 0.49µm fluorescent beads at 1x10^7 beads/ml in the absence (Control) or presence of CBD and AEA (each at 4µM). The average number (±SEM) of a) prey per ciliate cell and b) vacuoles per ciliate cell was determined over 180 min. n=3.

Table 3.3: Average Phase 1 ingestion rate (prey/cell/min) and lag phase (min) (±SEM) when *T. pyriformis* feeds on *Synechococcus* (Pico) or 0.49µm diameter beads (1x10^7 beads/ml) in the absence (Control) and presence of 4µM CBD (+CBD) or AEA (+AEA). Same trends seen with both prey particles. n=3 (beads), n=6 (Pico).

Treatment	Lag phase (min)	Ingestion rate (prey/cell/min)
Control (Pico)	00.00±0.00	1.23±0.05
CBD-Pico	59.10±0.27	2.33±0.31
AEA- Pico	31.30±0.37	1.00±0.09
Control (Beads)	00.00±0.00	1.80±0.26
CBD-Beads	58.80±0.19	2.33±0.19
AEA-Beads	36.40±0.44	1.77±0.11

3.4 Effect of CBD and AEA (4µM) on food vacuole passage time and defecation when *T. pyriformis* feeds on *Synechococcus*

This experiment was performed once and involved the monitoring of *Synechococcus*--containing food vacuoles in *T. pyriformis* over a 120 min period, with and without a 'chase' at 15 min (with/without CBD/AEA). The un-chased Control (Figure 3.4 – blue) behaved similarly to previous Controls in that vacuole formation was evident in Phase 1 (0-30 min), then vacuole formation stopped (30-55 min), then it started again in Phase 2 at a lower rate (Table 3.4). In the chased Control (Figure 3.4 – orange) the 1/50 dilution at 15 min was carried out in Chalkley's medium which contained no *Synechococcus,* hence it stopped further feeding/vacuole formation and only the persistence of the 3 pre-formed vacuoles were monitored thereafter. These 3 vacuoles persisted in the cell until 55 min (the vacuole Passage Time, VPT), after which they were defecated in a linear manner at a rate of 0.085±0.002 vacuoles/cell/min which was slower than the ingestion rate. All vacuoles were lost from the cells by 88 min (Figure 3.4).

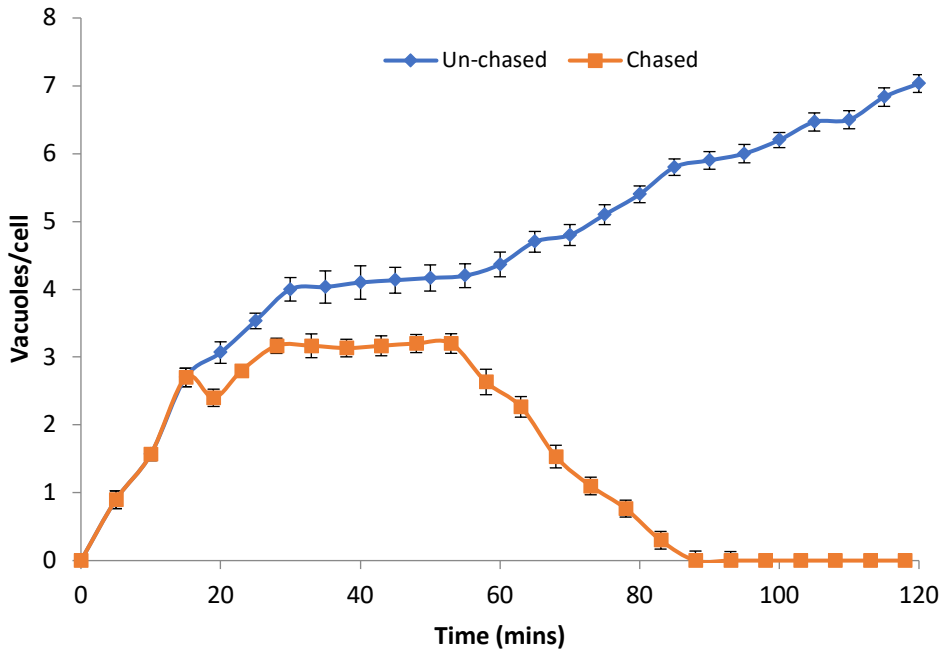

Figure 3.4: The average number of vacuoles/cell (±SEM) when *T. pyriformis* feeds on *Synechococcus* at 1x10^7 cells/ml, a) with no interruption ('un-chased') and b) when diluted 1/50 at 15 min ('chased'). n=3.

The chased Tests (Figure 3.5 – orange) showed a similar response to the Control (Figure 3.4 - orange). The presence of 4µM cannabinoid at 15 min did not significantly affect the vacuole passage time nor the defecation rates (Table 3.4); all cells needed *ca.* 12 min to defecate one vacuole.

The un-chased Tests (Figure 3.5 – blue) behaved similarly to previous Tests (Figure 3.3) in that the addition of AEA/CBD at 15 min immediately halted vacuole formation (at 3 V/C), whereas the Control continued to form a 4th vacuole by 30 min (Figure 3.4). Lag phases were shorter than previously reported (Table 3.2) but the trend was the same in that, CBD resulted in a significantly (Tukey's HSD, P<0.01) longer lag phase than AEA (Table 3.4).

Table 3.4: Feeding parameters (average±SEM) when *T. pyriformis* feeds on *Synechococcus* ($1x10^7$ cells/ml) in the absence (Control) and presence of 4µM CBD (+CBD) or AEA (+AEA) and when (i) the CBD/AEA is added at 15 min (Un-chased) or, (ii) when the culture is diluted 1/50 into Chalkley's medium containing CBD/AEA ('Chased'). Significantly different to control at P<0.05* or P<0.01** (Tukey's HSD). CBD significantly different to AEA at P<0.05^ or P<0.01^^ (Tukey's HSD). Phase 1 vacuole formation rate for the Control was determined between 0 and 30 min~. n=3.

Parameter	**Control**	**+CBD**	**+AEA**
0-15 min			
Vacuole formation rate, VFR (vacuoles/cell/min)	0.18±0.01	0.19±0.01	0.17±0.01
Post addition of cannabinoids in Tests			
Chased			
Vacuole passage time (min)	54.687±1.67	49.67±1.67	54.67±3.33
Defecation rate (vacuoles/cell/min)	0.088±0.00	0.08±0.01	0.09±0.01
Un-chased			
Lag phase (min)	0.000±0.000	45.00±0.00**^^	21.67±4.41**
Vacuole formation rate, VFR (vacuoles/cell/min) Phase 1	0.138±0.00~	0.617±0.01**^^	0.08±0.02*
Vacuole formation rate, VFR (vacuoles/cell/min) Phase 2	0.048±0.00	0.04±0.00	0.04±0.00

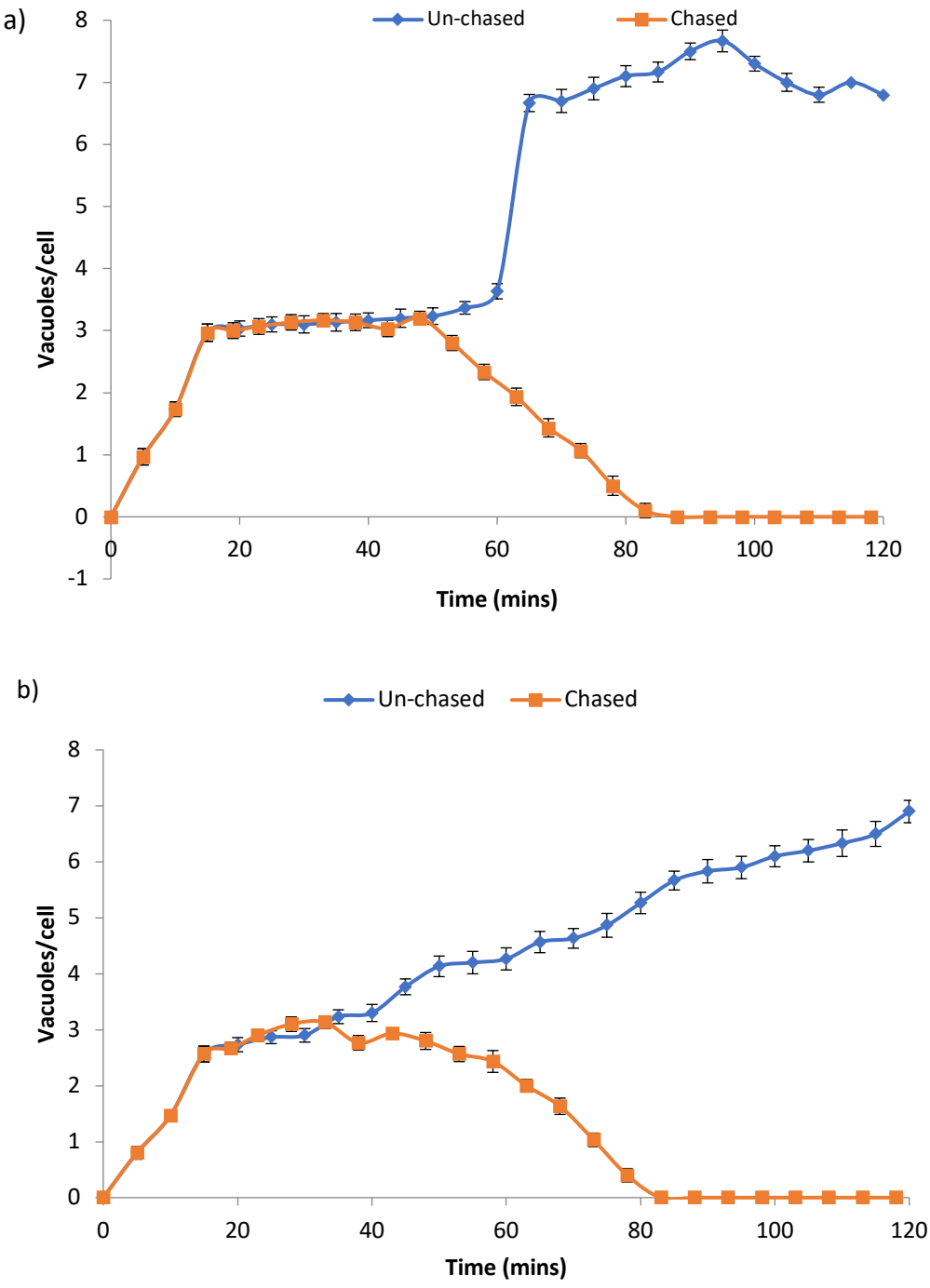

Figure 3.5: The effect of a) CBD and b) AEA on the average number of vacuoles/cell (±SEM) when *T. pyriformis* feeds on *Synechococcus* at $1x10^7$ cells/ml and when (i) 4µM AEA/CBD is added at 15 min (blue line) or, (ii) when the culture is diluted 1/50 into Chalkley's medium containing 4µM CBD/AEA (orange line). n=3.

After this lag, AEA-treated cells exhibited a short Phase 1 (40-50 min), a short break (50-60 min), followed by a longer Phase 2 (60-120 min) (Figure 3.5b). The Phase 1 vacuole formation rate (VFR) was significantly (Tukey's HSD, $P<0.05$) lower than that of the Control, but this time, rates were equivalent in Phase 2 (Table 3.4). CBD-treated cells exhibited a very short Phase 1 (60-65 min), a very short break (65-70 min), followed by a short Phase 2 (70-95 min) (Figure 3.5a). The Phase 1 VFR was significantly (Tukey's HSD, $P<0.01$) higher than those of the other systems (14x higher), resulting in 4 vacuoles being produced in 5 min. This rate was also 3-times higher than that reported for CBD in Table 3.2. The Phase 2 VFR was also equivalent to that of the Control and AEA-treated cells (Table 3.4).

Now knowing that vacuole defecation is occurring in Phase 2, the VFR in this Phase would be a Net rate (formation and defecation). Therefore, defecation rate was subtracted from this Net VFR, in each triplicate, to provide a Gross VFR for Phase 2. Resultant rates were remarkably similar and not significantly different to each other (ANOVA, $P=0.79$): 0.13±0.00, 0.12±0.01 and 0.13±0.01 vacuoles/cell/min for Control, CBD- and AEA-treated cells, respectively. These rates were equivalent (ANOVA, $P=0.625$) to the Phase 1 VFR of the Control (0.13±0.00 vacuoles/cell/min, Table 3.4); a Gross rate calculated over the first 30 min of feeding where no defecation of fluorescent vacuoles occurs due to their VPT being 55 min (Table 3.4). Thus, Control Phase 1 and Phase 2 Gross VFRs were equivalent and CBD/AEA did not appear to affect this Phase 2 rate.

3.5. Effect of CBD and AEA concentration on *T. pyriformis* feeding on *Synechococcus*

With the knowledge that CBD and AEA significantly affects Phase 1 of the ciliate feeding process, the effect of different concentrations of AEA and CBD on the feeding lag (if present) and instantaneous ingestion rates were examined (Figure 3.6). Two features were common to both AEA and CBD. Both caused a significant (ANOVA, $P<0.01$) reduction in ingestion rate (compared to the Control), with no lag, at 1.75µM and 2µM, then both caused a significant (ANOVA, $P<0.01$) lag from 2.25µM onwards (Figure 3.6). Differences were then evident at concentrations >2.25µM.

AEA-treated cells showed a gradual increase in both lag time and ingestion rate from 2.25µM until a plateau was reached at 3µM (Figure 3.6b) and where ingestion rate was

equivalent to the Control (ANOVA, P>0.05). CBD-treated cells maintained a lag of *ca*. 30 mins, with low ingestion rate, between 2.25µM and 3µM, and then both parameters increased gradually until they plateaued at 3.5/4µM (Figure 3.6b).

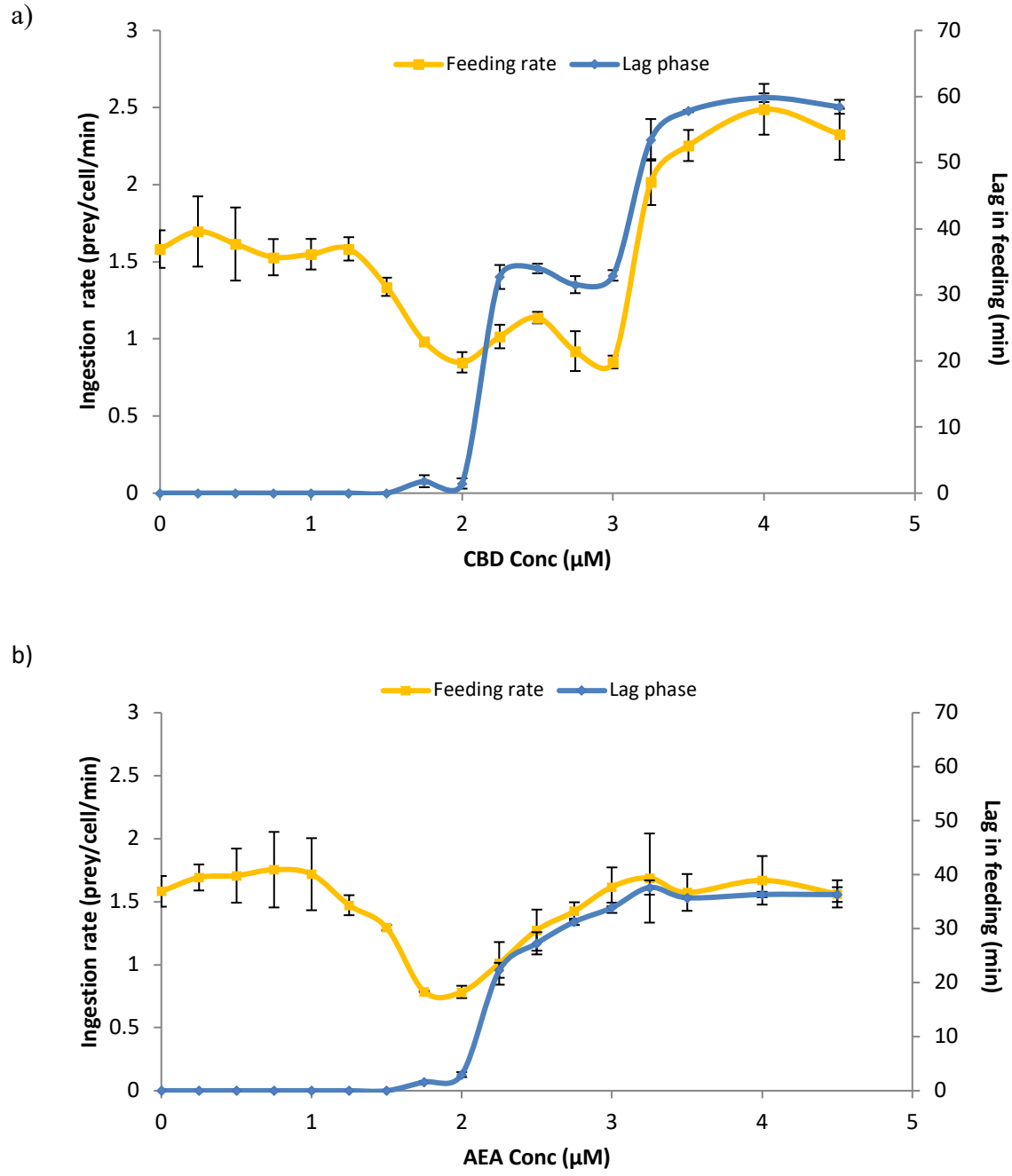

Figure 3.6: The effect of a) CBD and b) AEA concentration (µM) on (i) the duration of the lag phase and (ii) instantaneous ingestion rate (following that lag phase, if one is present), when *T. pyriformis* feeds on *Synechococcus* at 1x10^7 cells/ml. Data are averages (±SEM). n=3.

What is evident in both cases is that lag and ingestion rate patterns mirror each other very closely and there is a good correlation between them (Figure 3.7). This suggests that the feeding rate post lag, is a direct consequence of the length of that lag.

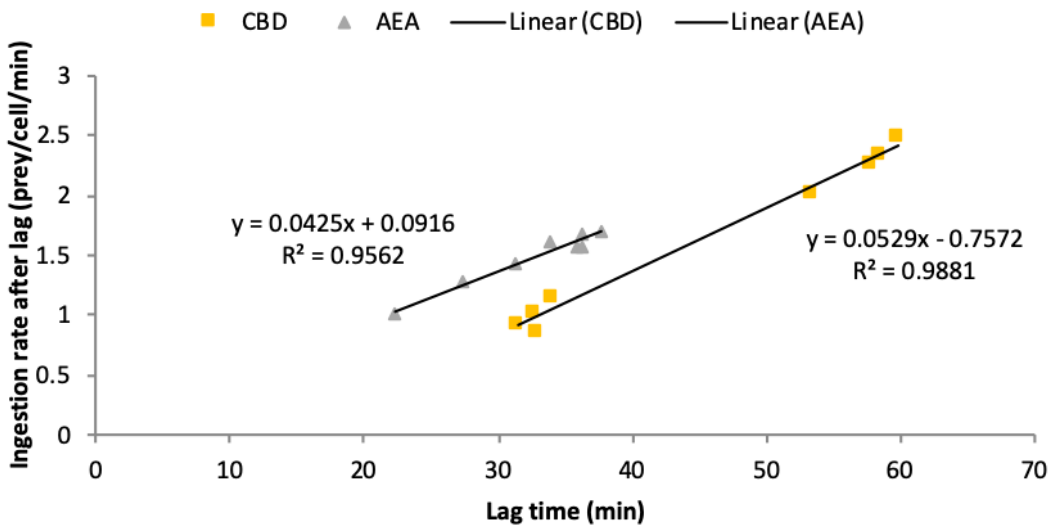

Figure 3.7: Relationship between the length of the cannabinoid-induced lag phase and subsequent instantaneous ingestion rate that follows, in *T. pyriformis,* using data in Figure 3.6. n=3.

3.6. Effect of blocking PPARα on CBD effects on *T. pyriformis* feeding on *Synechococcus*

The effect of blocking the PPARα receptor with GW6471 (10µM), on CBD (4µM) induced lag and feeding was tested. Results showed that the blocker alone had no effect on the ciliate ingestion, and it did not alleviate the lag or subsequent increased ingestion rate in the presence of CBD (Figure 3.8a).

Considering OEA is a natural ligand for PPARα, an additional experiment was performed to test whether OEA at its IC50 for *T. pyriformis* cell death (45µM, Wanlahbeh, 2020) affected feeding. Results showed that OEA had no effect, and hence the blocker (90µM) also had no effect (Figure 3.8b).

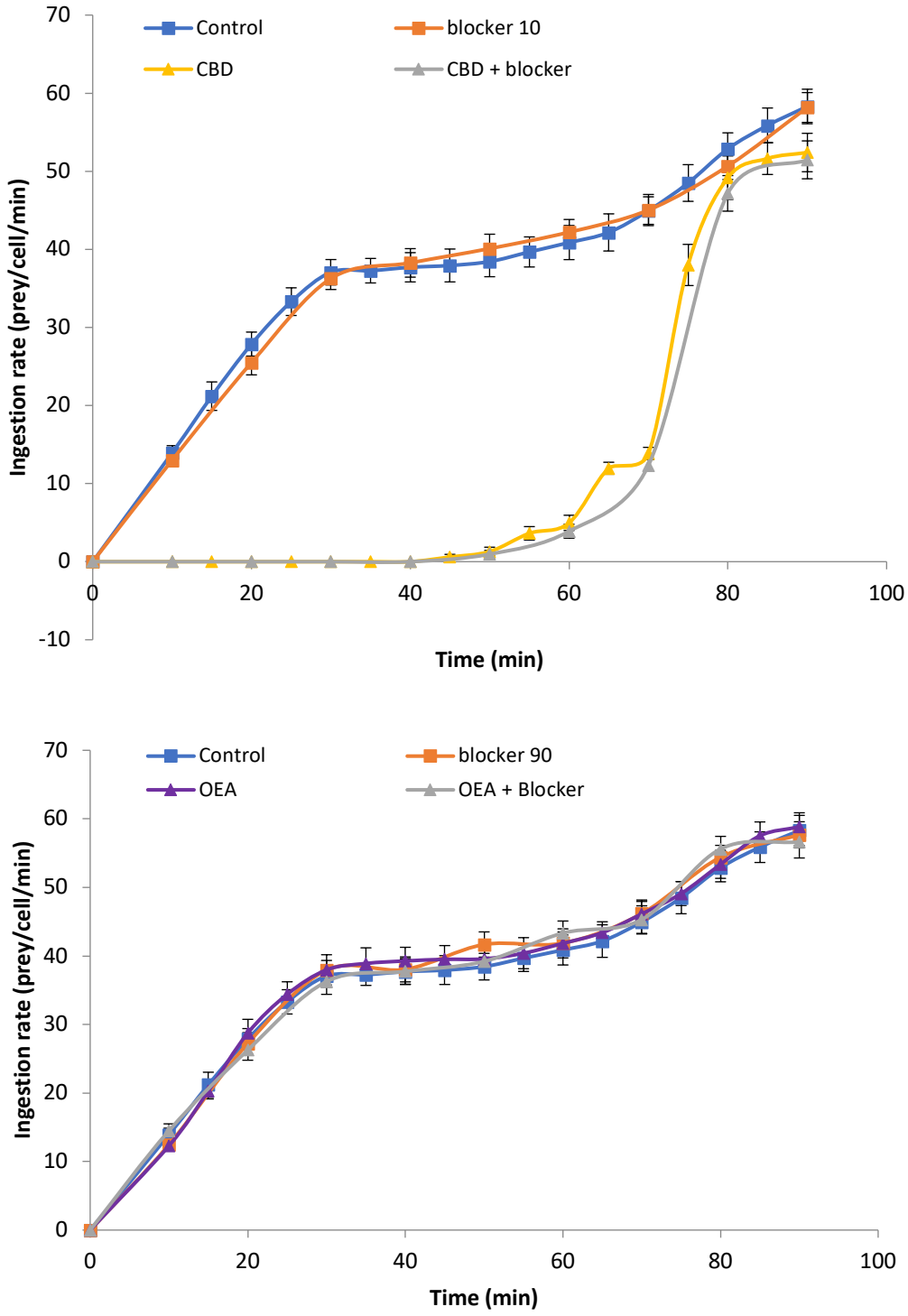

Figure 3.8: The effect of blocking PPARα with GW6471 on the feeding of *T. pyriformis* on *Synechococcus* at 1x10^7 cells/ml, a) in the presence of CBD, b) in the presence of OEA. Data are average ingestion rates (±SEM). 10 = blocker at 10µM, 90 = blocker at 90µM. n=6.

4. Discussion

4.1 Summary of major findings

The overall aim of this study was to examine the effect of exogenous CBD and AEA on prey ingestion and food vacuole formation in the ciliate *Tetrahymena pyriformis*. A naturally fluorescent bacterial prey was employed, *Synechococcus* sp., which is indigestible to this ciliate (Thurman et al., 2010) and hence remained visible throughout its journey from ingestion to defecation. In addition, this bacterium was shown to be unresponsive to CBD and AEA thus any effect of these cannabinoids on the ciliate would be a direct effect on the ciliate cell as opposed to it being an indirect effect of ingesting an affected prey.

The feeding dynamics of *T. pyriformis*, in the absence of cannabinoids, showed an initial bout of feeding (Phase 1), then a break, followed by a second bout of feeding (Phase 2), which had an ingestion rate that was significantly lower than that in Phase 1. Both CBD and AEA consistently affected Phase 1 only although this appeared to have nothing to do with food vacuole trafficking or defecation, as these were unaffected by both cannabinoids.

Both AEA and CBD caused a reduction in Phase 1 ingestion rate at 1.75µM and 2µM, and then a cessation in feeding at 2.25µM. The length of this lag was variable and the subsequent ingestion rate that followed appeared to reflect the duration of the lag, i.e., longer lag gave rise to increased ingestion rate. At 4µM, AEA cause a lag of 30-36 min followed by an ingestion rate that was equivalent to the control. CBD, on the other hand, caused a lag of *ca.* 60 min followed by an ingestion rate that was greater than the Control (hyperphagia). Neither the lag nor the hyperphagia caused by CBD were prevented by blocking the PPARα receptor.

4.2. Bacterial interactions with cannabinoids

The prey used in the current study was a freshwater cyanobacterium, *Synechococcus* sp. ('Pico 3'). This genus is characterized as a photosynthetic Gram-negative bacterium (Perkins et al., 1981) that, in addition to Chlorophyll *a*, contains the accessory light-harvesting pigments phycoerythrin and phycocyanin (Ficner and Huber, 1993). Freshwater species,

such as Pico 3, contain more phycocyanin than phycoerythrin, giving the culture a 'blue-green' appearance (Bryant, 1982; Six et al., 2007); marine species contain more phycoerythrin than phycocyanin, giving the culture a pink appearance (Six et al., 2007; Taylor et al., 2013).

It was important to investigate whether this bacterium responded to AEA and CBD itself, as if it did, then any effect of these cannabinoids on the ciliate might be due to an indirect effect of ingesting an affected prey, rather than being a direct effect on the ciliate. Data showed that *Synechococcus* concentration was not affected by CBD/AEA over a 180 min period (Table 3.1), suggesting it is unresponsive to these cannabinoids.

Cannabis sativa has long been recognized as possessing strong anti-bacterial properties (Appendino et al., 2011) however, Gram-positive bacteria have been shown to be more susceptible than Gram-negative bacteria. Crude extracts from *C. sativa* leaves can inhibit the growth of Gram-positive bacteria (*Staphylococcus aureus*) and, to a lesser extent, Gram-negative bacteria (*Escherichia coli, Pseudomonas aeruginosa, Vibrio cholerae*) (Lone and Lone, 2012; Mkpenie et al., 2012; Anjum, 2018). The observed antimicrobial activity has been attributed to polyphenols as there is a strong correlation between anti-microbial activity and polyphenol content of those extracts tested (Mkpenie et al., 2012). Polyphenols interact with the peptidoglycan in bacterial cell walls which is highly accessible in Gram-positive cell walls but covered by an extensive lipopolysaccharide (LPS) layer in Gram-negative cell wall which hinders the peptidoglycan-polyphenol interaction (Nohynek et al., 2006; Cui et al., 2012).

Studies that have examined the direct effect of cannabinoids on bacterial survival also show the trend of Gram-positive strains being more susceptible than Gram-negative strains but the mechanism behind this is unknown. Van Klingeren and Ham (1976) recorded minimum inhibitory concentrations (MICs) of 2-5µg/ml and 1-5µg/ml for Δ9-THC and CBD, respectively, against various strains of Gram-positive *Staphylococcus aureus* and streptococci (*Streptococcus pyogenes*, *S. milleri*, *S. faecilis*). The Gram-negative *Escherichia coli*, *Salmonella typhi* and *Proteus vulgaris* were considered resistant (MIC >100µg/ml). Using another cannabinoid, Cannabichromene (CBC), Turner and Elsohly (1981) recorded

MIC values of 0.78, 1.56 and 25µg/ml with the Gram-positive *Bacillus subtilis*, *S. aureus* and *Mycobacterium smegmatis*, respectively. Although the MICs for the Gram-negative *E. coli* and *Pseudomonas aeruginosa* were not reported, the authors stated that these strains were 'less sensitive'; indicating an MIC >25µg/ml (highest concentration tested). Appendino et al. (2008) compared the potency of *C. sativa*'s five main cannabinoids, CBC, CBD, Δ9-THC, Cannabigerol (CBG) and Cannabinol (CBN), against strains of methicillin-resistant *S. aureus* (MRSA). MIC values ranged from 0.5-1µg/ml (CBD), 0.5-2.0µg/ml (Δ9-THC), 1.0µg/ml (CBN) and 1.0-2.0µg/ml (CBC, CBG), which although very similar (*ca*. 1.6-6.4µM) suggesting that CBD is the most toxic of all five.

Results from the current study agree that a Gram-negative bacterial strain, *Synechococcus* sp., was not inhibited by CBD. The concentrations used (4 and 8µM) were close to the range of MICs recorded for Gram-positive cell susceptibility to CBD (Klingeren and Ham, 1976; Appendino et al., 2008). However, even though *Synechococcus* cell concentration was not affected, there might still be the possibility that the cannabinoids entered the cells and remained there. If this were the case, then any CBD/AEA within *Synechococcus* cells might indirectly affect the ciliate, post-ingestion. This was tested by pre-incubating *Synechococcus* with 4µM AEA/CBD for 1h, washing the cells and then feeding them to *T. pyriformis*. Results showed that these 'pre-loaded' cells were ingested at the same rate as untreated cells and there was no negative effect on the ciliate (Figure 3.1).

This lack of effect might have something to do with the fact that *Synechococcus* cells are indigestible to *T. pyriformis* (Thurman et al., 2010), i.e., lack of digestion would mean a lack of release of prey-harboured AEA/CBD in the ciliate's food vacuole. It would be interesting to repeat this pre-loading experiment with a digestible bacterial prey (which showed no obvious response to AEA/CBD based on cell survival) to see whether any cannabinoid is harboured by the bacterial cell and subsequently released into the ciliate cell upon prey digestion. It might be possible to test the extent of CBD harbouring in bacterial cells with the use of Fast Blue B salt reagent, in combination with thin layer chromatography (TLC); a dye which stains CBD orange and THC red (Ardrey, 2005). Binder and Meisenberg (1978) used this dye, and TLC, to monitor the metabolism of THC by 15 bacterial strains (strains of *Azotobacter, Bacillus, Proteus, Pseudomonas, Serratia* and *Streptomyces*). The Gram-

positive strains showed some ability to metabolise THC although this was highly variable and occurred to a lesser extent to that of fungi. The three Gram-negative strains did not metabolise THC. It would be useful to extend the study of Binder and Meisenberg (1978) to specifically evaluate whether CBD actually enters the cells of Gram-negative bacteria, as *Synechococcus* is itself Gram-negative.

However, for the current study, *Synechococcus* still represented a cannabinoid-unresponsive, fluorescent and indigestible prey which allowed its cells to be visualised inside the ciliate for the full duration of a 3h experiment.

4.3 *Tetrahymena pyriformis* feeding on *Synechococcus* in absence of CBD and AEA

In the current study, *T. pyriformis* exhibited no lag period before feeding commenced on *Synechoccocus* (Figure 3.2). Two phases of feeding were then recorded. There was an initial phase (Phase 1: 0-30 mins), followed by a period of no feeding (30-50 min), and then a second phase of feeding (Phase 2: from 50 min). The ingestion rate and vacuole formation rate in the second phase were significantly lower than the rates in Phase 1 (Table 3.2).

Such patterns in *T. pyriformis* feeding have been recorded previously at Lancaster (Jones, 2017; Ballard, 2018) but there is no information in the literature as to the reason behind this pattern; particularly the observed break in feeding. This might be because most published studies have focus on instantaneous ingestion rates only (*aka* 'Phase 1') and by using short incubation times (e.g. Jonsson, 1986) the feeding break and Phase 2 has not been observed. In those studies which have monitored prey ingestion over longer periods of time, longer sampling intervals (10 min) than those used in the current study (2 and 5 min) might have led to the two distinct phases, and break, being missed with an average ingestion rate (incorporating Phases 1 and 2, and break) being deduced instead (e.g. Chrzanowski and Šimek, 1990).

In the current study, results from the pulse-chase experiment, where vacuole trafficking and defecation were monitored, confirmed that defecation of prey was occurring in Phase 2. So, the calculated Phase 2 rate of the Control would be a Net rate (vacuole formation and defecation). When defecation rate was subtracted from this Net rate, the resultant Gross

rate was equivalent to that in Phase 1; which itself is a Gross rate calculated over the first 30 min of feeding where no defecation of fluorescent vacuoles occurs due to their VPT being 55 min (Table 3.4). Therefore, there appears to be no real change in vacuole formation rate between the Phases, it only looks that way because net rates are always presented, though not acknowledged, and pulse-chase experiments are not routinely performed alongside feeding experiments to determine Gross rates. Data therefore suggests that for a given prey, temperature, concentration etc., the rate of Gross vacuole formation might proceed at a defined rate (like a 'conveyor belt').

Published data on 'Phase 1' (instantaneous) feeding of ciliates on *Synechococcus*, for comparison purposes, are rare. Thurman et al. (2010) recorded a vacuole formation rate of 0.444±0.017 vacuoles/cell/min, and a corresponding defecation rate of 0.137±0.004 vacuoles/cell/min, with the same *T. pyriformis* strain as the current study (and temperature) but feeding on *Synechococcus* sp. S-KH5 at $2x10^7$ cells/ml. These rates are higher than those recorded in the current study (Table 3.4) possibly due to the use of a different prey strain, and a higher concentration. It does however confirm the finding in the current study, in that that defecation rate was slower than ingestion rate. It also demonstrates that ingestion/vacuole formation rate and, to a lesser extent, defecation rates are variable, and dependent on prey strain and concentration.

It is currently unknown as to why *T. pyriformis* would exhibit a break from feeding in-between Phases 1 and 2, but it might have something to do with the availability of food vacuole membrane, the volume of which is limited in a cell and needs to be constantly recycled (Fok et al., 1982; Plattner., 2010). The maximum volume of vacuole membrane in *T. pyriformis* can be crudely estimated from experimental data (Table 3.2) and by knowing the biovolume of a *Synechococcus* S-KH3 cell (0.588±0.031μm^3, Wong 2017). In the current study, at satiation (150 min), *T. pyriformis* contained *ca.* 8 vacuoles each containing *ca.* 12 cells when fed with $1x10^7$ *Synechococcus* cells/ml (Table 3.2). This equates to *ca.* 56μm^3 of vacuolar membrane needed to surround these prey cells. Jones (2017) and Ballard (2018), using the same *T. pyriformis* strain but with different concentrations of *Synechococcus* S-KH3 ($1x10^8$ and $2x10^7$ cells/ml, respectively) recorded, 6 vacuoles containing 15 prey (*ca*. 53μm^3 membrane) and 9 vacuoles containing 9 prey (*ca*. 48μm^3 membrane), respectively, at

satiation (30 and 70 min, respectively). This suggests that only *ca.* 48-56µm^3 of membrane is available for food vacuole manufacture in this strain of *T. pyriformis*. The author cannot find any published estimates of the volume of available food vacuole membrane in any protistan cell, to which this estimate could be compared.

All *T. pyriformis* cultures in the current study were 3-days old, having been fed on *K. aerogenes*, and would be in their mid/late stationary phase of growth at the start of an experiment (Parry, personal communication). It is likely that the full amount of membrane for vacuole formation to enclose newly ingested *Synechococcus* would not be available, due to the presence of pre-existing food vacuoles containing non-fluorescent *K. aerogenes* cells. It is therefore hypothesised that, in the current study, all the available membrane was used to ingest *Synechococcus* in Phase 1 (between 0-30 min) and deposit them into four new food vacuoles. But when this membrane became unavailable (at 30 min), ingestion ceased; suggesting the ciliate cells already contained 4 pre-existing food vacuoles (8 vacuoles/cell = satiation, Table 3.2). Under these circumstances the cell would have to wait for pre-existing vacuoles to be defecated at the cytoproct so that their membrane could be recycled, to allow ingestion to start again (after 50 min). Based on the length of time of this feeding break (20 min), this might involve the defecation of one pre-existing vacuole (takes 12 minutes, Table 3.4) with a further 8 minutes being necessary for the recycling process to be complete, although the author can find no published data on how long the recycling process actually takes in protistan cells. Future experiments could stain *T. pyriformis* cells at $Time_{zero}$ with 4,6-Diaminide-2-phenylindole dihydrochloride (DAPI) to visualise ingested *K. aerogenes* and determine the number pre-existing food vacuole in cells, to see if there is a relationship between 'fullness' and the observed ingestion dynamics.

4.4 The effects of CBD and AEA on *Tetrahymena pyriformis* feeding

The feeding of *T. pyriformis*, on *Synechococcus* and fluorescent beads, was examined in the presence of 4µM CBD and AEA. This concentration was chosen as it is close to the IC50 values for both compounds when tested against this *T. pyriformis* strain (CBD, 4.38µM, AEA, 3.78µM, Jones 2017). Results showed that neither cannabinoid affected the trafficking of food vacuoles in the ciliate cell nor did they affect the Gross vacuole formation in Phase 2. At satiation they had no significant effect on prey/cell and even though significance was

found for lower vacuoles/cell with higher prey content in their presence, data were incredibly similar.

The only phase that was obviously affected by the cannabinoids, was the initial phase of ingestion/vacuole formation (Phase 1) (Figure 3.6). Here, both caused the complete cessation of ciliate feeding for a given period of time (feeding lag), with CBD inducing a significantly longer lag (*ca.* 60 min) than AEA (*ca.* 36 min) at 4µM. Following this lag, feeding resumed and AEA-treated cells had equivalent rates to the Control by 3µM, while CBD-treated cells had increased rates (hyperphagia) compared to those of the Control and AEA-treated cells by 3.5µM (Figure 3.6).

4.4.1 Effect on CBD and AEA on *T. pyriformis* capacity to feed

Both cannabinoids stopped *T. pyriformis* feeding for a given amount of time (the lag) (Figures: 3.2, 3.3, 3.5 3.6, 3.8 and Tables: 3.2, 3.3, 3.4) but the mechanism behind this is currently unknown. One possibility was that the lag was related to cell death, since 4µM of either cannabinoid would induce the death of *ca.* half the population by 90 min (Jones, 2017). However, for CBD at least, this does not seem to be the case and the feeding lag appears to be independent of cell death. Firstly, the dose response experiment showed that a concentration of 2.25µM was required to induce a lag (feeding was reduced at 1.75 and 2µM) (Figure 3.6). CBD does not induce cell death in *T. pyriformis* until 3.16µM (the MIC) (Jones, 2017), thus the observed induction of the lag (and reduction in feeding) occurred in the absence of cell death. Secondly, *T. pyriformis* cell death can be completely prevented by blocking the PPARα receptor (Wanlahbeh, 2020). In the current study, the blocking of this receptor had no effect on the lag phase (or feeding rate) of *T. pyriformis* in the presence of 4µM CBD (Figure 3.8), suggesting different targets are used by CBD for causing cell death and affecting feeding.

The case for AEA not being associated with cell death is less strong. It mirrored the action of CBD in that a lag was induced at 2.25µM (and feeding was reduced at 1.75 and 2µM) (Figure 3.6). But its MIC is lower, being 1.17µM (Jones, 2017) and therefore, unlike CBD, the AEA effects on lag (and feeding) at these concentrations would be accompanied by cell death. Secondly, Wanlahbeh (2020) showed that blocking PPARs had no effect on AEA induced cell

death and because she did not identify the receptor involved, the current study could not block a 'death-receptor' to see if it also stopped the effect on feeding.

One thing that is common to both cannabinoids is that *T. pyriformis* cell death in the presence of any concentration of AEA/CBD only occurs for 90 min, after which cells start to recover (Wanlahbeh, 2020). This response has been observed previously with *T. pyriformis* in the presence of Δ9-THC but the time taken for the start of recovery was not stated (McClean and Zimmerman, 1976). Neither CBD nor AEA induced a lag of 90 min to correlate with the length of population cell death. Also, when feeding resumed after their *ca*. 30-36 or 60 min 4µM-induced lag, respectively, cells would have still been dying. This, although not as strong a case as CBD, suggests that the action of AEA on the feeding process might also be independent of cell death but further work is necessary to confirm this.

With the knowledge that the cannabinoid effect of feeding is possibly independent of cell death and considering AEA and CBD both instigate a lag at the same concentration (2.25µM), it suggests that they might be acting on the same target with equivalent efficacy. If they did, the difference in lag times they induce might then be related to the capacity of *T. pyriformis* to degrade these cannabinoids within the cell.

A FAAH-like enzyme is known to metabolise AEA in *T. pyriformis* and *T. thermophilia* (Karava et al., 2001, 2005). Moreover, Anagnostopoulos et al. (2010) showed that even though the FAAH in *T. thermophila* could hydrolyse all of its endogenous NAEs, the highest enzyme activity was evident with AEA even though it was the least abundant NAE in the cell. At 100 µM AEA, *ca.* 10^6 *T. thermophila* cells/ml hydrolysed 4.9 nmol AEA in 1 min at possibly 27°C (temperature inferred but not stated) (Anagnostopoulos et al., 2010). This suggests the ciliate population would require a period of 204 min to fully hydrolyse 1µM AEA at this temperature. Estimates for other cell types are rare but Kaczocha et al. (2006) showed that 10^6 rat basophilic leukaemia cells (RBL-2H3) hydrolysed 89% of AEA (0.1µM) in 5 min at 37°C. This suggests the population would require a period of 56 min to fully hydrolyse 1µM AEA at this temperature. The current study tested 1µM AEA (Figure 3.6) at 23°C with *ca.* 10^5 cells (Section 2.1.2) and found no effect of AEA on lag induction (or feeding), even though

AEA would have been present in the cell as its hydrolysis would be even slower than those calculated above.

There are currently no reports on the metabolism of CBD within ciliate cells. In humans, CBD is metabolised by cytochrome P450 (CYP450) oxidases, sulfotransferases and glucuronyl transferases (Ujváry and Hanus, 2016). Homologues of the first two are present in *T. thermophila* (www.ciliate.org) however only CYP450 oxidases have been thoroughly studied in other cells. Cytochromes P450 (CYPs) are a family of enzymes containing heme as a cofactor that function as monooxygenases (Jeffreys et al., 2018). In mammals, CYP450s are necessary for the detoxification of foreign chemicals and the metabolism of drugs (Šrejber et al., 2018). Even though there are more than 50 CYP450 enzymes, only six of them (CYP1A2, CYP2C9, CYP2C19, CYP2D6, CYP3A4, and CYP3A5) are responsible for metabolising 90 percent of medicinal drugs, including CBD (Lynch and Price, 2007). CBD undergoes extensive hydroxylation and further oxidations by these enzymes which results in some 100 CBD metabolites with the major metabolites being derivatives of CBD-7-oic acid (7-COOH-CBD) (Ujváry and Hanus, 2016). *T. thermophila* contains two CYP homologues, i.e., CYP13A1 (WBGene00011677) and CYP13A3 (WBGene00011675) (www.ciliate.org). These are members of the CYP13 family which is a member of the CYP3 clade (Yan and Cai, 2010), within which CYP3A4 and CYP3A5 are two of the six important CYPs for the metabolism of CBD. Thus, it is conceivable that *Tetrahymena* has the ability to metabolise CBD, but this has yet to be tested. Future work could include exogenous FAAH and CYPs into the feeding experiments to see if these reduce the extent of the feeding lag.

It is therefore unlikely that the mere presence of AEA or CBD in *T. pyriformis* cells induces a feeding lag, so they must be reacting with something, such as a protein, to cause this effect. Identifying their target is difficult, but the first stage would be to discern what stage in the feeding process was being affected by them. The fact that neither affected the trafficking of fully-formed vacuoles through the cell, or their defecation rate (Table 3.4), suggests that their target is either, (i) vacuole recycling from cytoproct to cytostome and/or the formation of a new phagocytic cup thus preventing any ingestion of captured prey or, (ii) prevention of prey capture, which is possibly receptor-mediated, so there is nothing to ingest into an awaiting phagocytic cup. Separating out the processes of prey capture and ingestion is

difficult as both are so closely coupled and prey/cell or vacuole/cell will not increase if either one is impaired. However, examination of the ingestion rates in the presence of these cannabinoids might offer some clue as to which stage of the process is most likely the target.

4.4.2 Effect of CBD and AEA on *T. pyriformis* ingestion rates

Both cannabinoids caused a reduction in feeding at 1.75 and 2µM with no lag ('direct effect') and then, when a lag was present, the subsequent ingestion rate increased and correlated strongly with the duration of this lag, i.e., the longer the lag the higher the ingestion rate afterwards (Figure 3.7). The latter response therefore appears to be a 'domino effect' with changes in ingestion rate being a consequence of the lag period duration ('indirect effect').

The direct effect was equivalent between CBD and AEA (MIC >1.5<1.75µM), after which analysis was complicated by the presence of a lag phase, and its own indirect effect on feeding. This experiment was only performed once and requires repeating to confirm the data. But, numerous experiments with 4µM did confirm that a lag does occur and that this differs between AEA and CBD with regards to its duration and rate of feeding afterwards.

With regards to this 'indirect effect', it could be due to either of the two potential cannabinoid targets in the feeding process, i.e., prevention of vacuole recycling or prey capture. If CBD/AEA completely stopped vacuole recycling/phagocytic cup formation, but prey capture was unaffected, *T. pyriformis* cells might accumulate prey at the cytostome during the lag period. When vacuole membrane then became available, more prey would be present (locally) to give rise to higher ingestion rates (compared to the cannabinoid-induced low rate). However, there are some observations which question this hypothesis. The first questions whether there would be enough food vacuole membrane available at the cytostome to capture this higher number of prey, if recycling had been completely halted beforehand. When examining the feeding behaviour of Control cells (Figures 3.2, 3.4) the break in feeding between Phase 1 and Phase 2 was considered to be due to a lack of available membrane (cells were 'full'); these cells would have had a fully functional capture mechanism (Section 4.3). However, <u>if</u> prey cells had accumulated at the cytostome of these

Control cells, why was the Gross ingestion rate after the break (in Phase 2) not higher than that in Phase 1? This suggests that membrane recycling is governing the process of ingestion, even if prey capture is enhanced.

The second observation relates to the rate of this membrane recycling. It would be expected that if AEA- and CBD-treated cells fully recovered after the lag period, this rate would be equivalent in each of the treated cells so subsequent ingestion rate should also be equivalent. This was not recorded. For example, when a 30 min lag was induced (Figure 3.6), AEA-treated cells had a post-lag ingestion rate of *ca.* 1.5 prey/cell/min, which was higher than those at 1.75 and 2µM and thus conformed with the hypothesis. CBD-treated cells, on the other hand, had a post-lag ingestion rate of *ca.* 1 prey/cell/min which was significantly lower than that of AEA-treated cells ($P<0.05$) and equivalent to those at 1.75 and 2µM CBD; no increase in rate which does not conform to the hypothesis. The final observation is that when counting prey ingestion in *T. pyriformis* cells, the author has never seen an obvious accumulation of fluorescent *Synechococcus* cells at the cytostome in cannabinoid-treated cells.

There is also much evidence to suggest a similarity between the cellular machinery required for recycling/phagocytic cup formation and vacuole trafficking, and the latter was shown to be unresponsive to AEA or CBD treatment. Studies on the ciliate *Paramecium* have confirmed that actin microfilaments are associated with phagocytosis (Cohen et al., 1982), playing a role in the formation of the phagocytic cup, migration of newly formed food vacuoles into the cell and fusion with acidic-lysosomes (Allen and Fok, 1983 a-c). Actin microfilaments have also been shown to play a role in the formation of food vacuoles (Tiggemann and Plattner, 1981; Tiggemann et al., 1981) and their transit in *Tetrahymena,* after binding to heavy meromyosin (HMM- proteolytic fragment of myosin) (Méténier, 1984). Being involved in both the trafficking and formation of vacuoles renders actin an unlikely target for AEA and CBD.

Another element that may be inclusive in the ciliates' cytoskeleton is Dynamin. Although it is yet unclear the exact methodology and involvement of dynamin in phagocytosis in different organisms; previous studies have indicated that it may contribute to the actin-

dependent processes involving actin-binding protein 1 (ABP1) in mammals (Kessels et al., 2001) and yeast (Rooij et al., 2010). In mammalian cells, it has been observed that knocking out Dynamin 1 and 2 leads to elongated microtubules which do not pinch off and cannot be stabilized by F-actin, which is essential for phagosome processing (Ferguson et al., 2009). Lack of Dynamin A in *Dictyostelium* cells has shown defects in acidification process carried out by lysosomal enzymes as well as the binding of early phagosomes which is mediated by F-actin (Gopaldass et al.,2011) Dynamin 2 has also demonstrated involvement in the phagocytosis process in macrophages (Gold et al., 1999), particularly regulating the vacuole processing (exocytosis) during phagocytic cup formation (Di et al., 2003). Considering that the latter is not affected by AEA or CBD it is unlikely that recycling/cup formation is affected also. If it was, the target would be a distinctly different component of the cytoskeleton.

On balance, it appears that the more likely candidate target might be the process of prey capture. If prey capture completely stopped, but vacuole recycling/phagocytic cup formation was unaffected, cells would accumulate membrane at the cytostome (since vacuole trafficking and defecation would be occurring); but prey would still not be ingested. Then, when prey capture resumed, ingestion could proceed at a rate determined by the amount of accumulated membrane available at the cytostome. The limiting factor for ingestion might then be prey capture. If this were so, it would be expected that, at a given prey concentration and temperature, ingestion rates between experiments would be equivalent. In the current study Phase 1 ingestion rates were variable even though a standard prey concentration of $1x10^7$ *Synechococcus* cells/ml at a temperature of 23^{o}C was used, i.e., 1.23±0.05 prey/cell/min (Table 3.2), 1.80±0.26 prey/cell/min (Table 3.3), 1.58±0.12 prey/cell/min (Figure 3.6) and 1.19±0.04 prey/cell/min (Figure 3.8). Such differences using a single prey concentration have been observed by others and the accepted explanation is that it is due to variations in the nutritional and physiological conditions of the protist at the start of the experiment, i.e., starved cells feed faster than well-fed cells (Boenigk et al., 2001). Although *T. pyriformis* was grown on *K. aerogenes* for 3 days prior to each experiment, the level of prey was not standardised and thus, slight variations in their 'fullness' would be expected at the start of experiments. However, what is evident is that ingestion rate (possibly via capture) adjusts very quickly to exploit whatever membrane is available.

4.4.3 Possible targets within *T. pyriformis* for AEA and CBD

It is hypothesised that AEA and CBD completely stops prey capture but that pre-existing vacuoles are trafficked and defecated as normal, and membrane is recycled to the cytostome where it accumulates. A lag of 60 min would allow the accumulation of more membrane than a 30 min lag and is the possible reason as to why ingestion rates of the former are higher (with CBD). However, there currently is no explanation as to why a lag of 30 min would result in significantly different ingestion rates (*ca.* 1.5 and 1.0 prey/cell/min for AEA- and CBD-treated cells, respectively) - unless the effect of AEA is completely lost by 30 min whereas CBD is still partially effective at 30 min.

Future work should examine the interaction between cannabinoids and those receptors associated with prey capture. To date, C-type lectins have been shown to be involved in protist feeding (Bracha et al., 1982; Allen and Davidowicz, 1990; Alsam et al. 2005; Wootton et al., 2007) and recent studies at Lancaster University have confirmed the presence of C-type lectins for Mannose, GalNAc and GlcNAc in *T. pyriformis* (Boboc, 2020) and in the amoeba *Vermamoeba vermiformis* (Al-hammadi, 2020). The latter study also examined the interaction between CBD and these receptors as, in a similar manner to the current study, CBD disrupts the feeding of the amoeba on *Synechococcus* by inducing a feeding lag. Blocking each C-type lectin in turn (with mannose, GalNAc and GlcNAc), in the presence and absence of CBD, revealed no interaction between CBD and those receptors for GalNAc or mannose. However, there was an interaction with the GlcNAc receptor; when this receptor was blocked in the presence of CBD the extent of the feeding lag was doubled. However, Al-hammadi (2020) did not consider CBD to physically bind to the GlcNAc receptor, only that the yet unidentified 'CBD target' and the GlcNAc receptor are both involved in vacuole formation (as opposed to being involved in prey capture which appeared to be the sole role of the mannose and GalNAc receptors). And, because all the cytoskeleton machinery is in place for vacuole formation in *V. vermiformis* (and is not directly affected by CBD), Al-hammadi (2020) considered the 'CBD target' to lie within the signalling cascade which stimulates the cytoskeleton to form the phagocytic cups.

Repeating such experiments with *T. pyriformis* would allow an evaluation as to whether CBD interacts with C-type lectins in the same way as *V. vermiformis* or whether it is prey capture

itself that is affected by CBD. And, considering that scavenger receptors have recently been identified in *D. discoideum* (Sattler et al., 2018), it would be beneficial to evaluate whether *T. pyriformis* possesses such feeding receptors and if it does, whether they interact with CBD.

5. Conclusions

Previous research has indicated that the ciliate *Tetrahymena* possesses a rudimentary endocannabinoid system but the effect on feeding, and the molecular target for a cannabinoid remained unstudied. The current study assessed the former, using AEA and CBD as examples of endo- and phyto-cannabinoids, respectively. The results showed that both of these compounds could modify the feeding behaviour of *Tetrahymena*, principally by inducing a lag before feeding resumed. The lengths of these lags were different at 4µM (CBD *ca.* 60mins, AEA *ca.* 36mins), suggesting that CBD is a more potent cannabinoid than AEA. This might be due, in part, to faster metabolism of AEA (with the FAAH-like enzyme) compared to CBD (with possibly CYP13 enzymes). Following the lag, the ingestion rates for the AEA-treated cells return to the same state as the Control, whereas CBD induced hyperphagia.

Neither of the cannabinoids affected the trafficking of the food vacuoles or their defecation rate, therefore the potential target candidates were narrowed down to (i) vacuole recycling, and formation of the new phagocytic cup or (ii) prevention of prey capture. Since much of the machinery used for the former are also used to traffic vacuoles, it was considered unlikely that this would be the target, and that it is the stage of prey capture that is affected. However further work should confirm this as CBD might be affecting the signalling cascade that initiates phagocytic cup formation, which was not considered here and only came to light after submission of this thesis.

6. Acknowledgements

First and foremost, I would like to sincerely thank my principal academic supervisor, Dr Jackie Parry. I am so grateful for her continuous support, patience, advice and guidance throughout the journey of this project, development of my thesis and beyond. Many thanks and gratitude to my second academic supervisor, Dr Karen Wright, for her kind advice support and input during my research. Extended thanks go to Janice Drinkall and my colleagues; Adela, Nadia and Israa for all their assistance and encouragement during my time in the laboratory.

And I would also like to pay my special regards to all those that are close to me;

My parents: Upender and Kamleash for giving me strength, independence and backing my academic choices.
My Siblings: Lucky and Sakshi for having faith in me, encouraging me to do better and simply just being there.
My Di: Babita for always being my 'go-to' person and bringing me a piece of home with you.
My Best friends: Sadhu and Maria for bringing a balance of madness and meditation in my life and being my personal cheer leaders.
And my beloved dog: Cutie for all the unconditional love and being my silent companion throughout the write-up of my thesis. 🐾

Thank you for supporting me every step of the way and helping me create many memories during my time at Lancaster, that I will cherish and hold onto.

7. References

Adl, S., Leander, B., Simpson, A., Archibald, J., Anderson, O., Bass, D., Bowser, S., Brugerolle, G., Farmer, M., Karpov, S., Kolisko, M., Lane, C., Lodge, D., Mann, D., Meisterfeld, R., Mendoza, L., Moestrup, ., Mozley-Standridge, S., Smirnov, A. and Spiegel, F. (2007). Diversity, nomenclature, and taxonomy of Protists. *Systematic Biology*, 56(4), pp.684-689.

Ahn, K., McKinney, M. and Cravatt, B. (2008). Enzymatic pathways that regulate endocannabinoid signaling in the nervous system. *Chemical Reviews*, 108(5), pp.1687-1707.

Ahn, S., Yi, S., Seo, W., Lee, M., Song, Y., Baek, S., Yu, J., Hong, S., Lee, J., Shin, D., Jeong, L. and Noh, M. (2015). A cannabinoid receptor sgonist N-Arachidonoyl Dopamine inhibits adipocyte differentiation in human mesenchymal stem cells. *Biomolecules & Therapeutics*, 23(3), pp.218-224.

Aizpurua-Olaizola, O., Elezgarai, I., Rico-Barrio, I., Zarandona, I., Etxebarria, N. and Usobiaga, A. (2017). Targeting the endocannabinoid system: future therapeutic strategies. *Drug Discovery Today*, 22(1), pp.105-110.

Al-hammadi, I. (2020). Actions of cannabinoids on amoebae. PhD Thesis, Lancaster University.

Allen, P. and Dawidowicz, E. (1990). Phagocytosis in *Acanthamoeba*: II. Soluble and insoluble mannose-rich ligands stimulate phosphoinositide metabolism. *Journal of Cellular Physiology*, 145(3), pp.514-521.

Allen, R. and Wolf, R. (1974). The cytoproct of *Paramecium caudatum*: structure and function, microtubules, and fate of food vacuole membranes. *Journal of Cell Science*, 14(3), pp.611-631.

Allen, R. and Fok, A. (1980). Membrane recycling and endocytosis in *Paramecium* confirmed by horseradish peroxidase pulse-chase studies. *Journal of Cell Science*, 45(1), pp.131-145.

Allen, R. and Fok, A. (1983a). Phagosome fusion vesicles of *Paramecium*. I. Thin-section morphology. *European Journal of Cell Biology*, 29(2), pp.150-8.

Allen, R. and Fok, A. (1983b). Phagosome fusion vesicles of *Paramecium*. II. Freeze-fracture evidence for membrane replacement. *European Journal of Cell Biology*, 29(2), pp.159-65.

Allen, R. and Fok, A. (1983c). Non-lysosomal vesicles (acidosomes) are involved in phagosome acidification in *Paramecium*. *The Journal of Cell Biology*, 97(2), pp.566-570.

Alenton, R., Koiwai, K., Miyaguchi, K., Kondo, H. and Hirono, I. (2017). Pathogen recognition of a novel C-type lectin from *Marsupenaeus japonicus* reveals the divergent sugar-binding specificity of QAP motif. *Scientific Reports*, 7(1), pp.1-9.

Anagnostopoulos, D., Rakiec, C., Wood, J., Pandarinathan, L., Zvonok, N., Makriyannis, A. and Siafaka-Kapadai, A. (2010). Identification of endocannabinoids and related N-acylethanolamines in *Tetrahymena*. A new class of compounds for *Tetrahymena*. *Protist*, 161(3), pp.452-465.

Anjum, M. (2018). Evaluation of antimicrobial activity and ethnobotanical study of *Cannabis sativa* L. *Pure and Applied Biology*, 7(2) pp.706-712.

Appendino, G., Chianese, G. and Taglialatela-Scafati, O. (2011). Cannabinoids: Occurrence and medicinal chemistry. *Current Medicinal Chemistry*, 18(7), pp.1085-1099.

Appendino, G., Gibbons, S., Giana, A., Pagani, A., Grassi, G., Stavri, M., Smith, E., Rahman, M.M. (2008). Antibacterial cannabinoids from Cannabis sativa: a structure−activity study. *Journal of National Products,* 71(8), pp. 1427–1430

Ardrey, R.E. (2005). Forensic Sciences – Thin layer chromatography. *In*, Encyclopedia of Analytical Science, Second Edition, Worsfold, P., Townshend, A., Poole, C. (eds), Eslevier.

Artmann, A., Petersen, G., Hellgren, L., Boberg, J., Skonberg, C., Nellemann, C., Hansen, S. and Hansen, H. (2008). Influence of dietary fatty acids on endocannabinoid and N-acylethanolamine levels in rat brain, liver and small intestine. *Biochimica et Biophysica Acta (BBA) - Molecular and Cell Biology of Lipids*, 1781(4), pp.200-212.

Bakas, T., van Nieuwenhuijzen, P., Devenish, S., McGregor, I., Arnold, J. and Chebib, M. (2017). The direct actions of cannabidiol and 2-arachidonoyl glycerol at GABA A receptors. *Pharmacological Research*, 119(Edition: 2017), pp.358-370.

Baker, D., Pryce, G., Davies, W. and Hiley, C. (2006). In silico patent searching reveals a new cannabinoid receptor. *Trends in Pharmacological Sciences*, 27(1), pp.1-4.

Ballard, H. (2017). An investigation into the effects of the cannabinoids Cannabidiol (CBD) and Anandamide (AEA) on the feeding behaviour of *Tetrahymena pyriformis*. Dissertation, Lancaster University.

Bär, A.-K., Phukan, N., Pinheiro, J. and Simoes-Bärbosa, A. (2015). The Interplay of host microbiota and parasitic protozoans at mucosal interfaces: Implications for the outcomes of infections and diseases. *PLOS Neglected Tropical Diseases*, 9(12), pp. 4176-9.

Baranova, I., Kurlander, R., Bocharov, A., Vishnyakova, T., Chen, Z., Remaley, A., Csako, G., Patterson, A. and Eggerman, T. (2008). Role of human CD36 in bacterial recognition, phagocytosis, and pathogen-Induced JNK-mediated signaling. *The Journal of Immunology*, 181(10), pp.7147-7156.

Basavarajappa, B. (2007a). The endocannabinoid signalling system: A potential target for next- generation therapeutics for alcoholism. *Mini-Reviews in Medicinal Chemistry*, 7(8), pp.769-779.

Basavarajappa, B. (2007b). Critical enzymes involved in endocannabinoid metabolism. *Protein & Peptide Letters*, 14(3), pp.237-246.

Baylie, R. and Brayden, J. (2010). TRPV channels and vascular function. *Acta Physiologica*, 203(1), pp.99-116.

Beltramo, M. and Piomelli, D. (2000). Carrier-mediated transport and enzymatic hydrolysis of the endogenous cannabinoid 2-arachidonylglycerol. *NeuroReport*, 11(6), pp.1231-1235.

Bergamaschi, M., Queiroz, R., Chagas, M., de Oliveira, D., De Martinis, B., Kapczinski, F., Quevedo, J., Roesler, R., Schröder, N., Nardi, A., Martín-Santos, R., Hallak, J., Zuardi, A. and Crippa, J. (2011). Cannabidiol reduces the anxiety Induced by simulated public speaking in treatment-naïve social phobia patients. *Neuropsychopharmacology*, 36(6), pp.1219-1226.

Bih, C., Chen, T., Nunn, A., Bazelot, M., Dallas, M. and Whalley, B. (2015). Molecular targets of cannabidiol in neurological disorders. *Neurotherapeutics*, 12(4), pp.699-730.

Bilici, R. (2014). Synthetic cannabinoids. *Northern Clinics of Istanbul*, 1(2), pp.121-126.

Binder, M. and Meisenberg, G. (1978). Microbial transformation of cannabinoids. *European Journal of Applied Microbiology and Biotechnology*, 5(1), pp.37-50.

Bisogno, T., Sepe, N., Melck, D., Maurelli, S., Petrocellis, L. and Di Marzo, V. (1997). Biosynthesis, release and degradation of the novel endogenous cannabimimetic metabolite 2-arachidonoylglycerol in mouse neuroblastoma cells. *Biochemical Journal*, 322(2), pp.671-677.

Bisogno, T., Maccarrone, M., De Petrocellis, L., Jarrahian, A., Finazzi-Agrò, A., Hillard, C. and Di Marzo, V. (2001). The uptake by cells of 2-arachidonoylglycerol, an endogenous agonist of cannabinoid receptors. *European Journal of Biochemistry*, 268(7), pp.1982-1989.

Bisogno, T., Melck, D., Petrocellis, L. and Marzo, V. (2008). Phosphatidic acid as the biosynthetic precursor of the endocannabinoid 2-arachidonoylglycerol in intact mouse Neuroblastoma Cells Stimulated with Ionomycin. *Journal of Neurochemistry*, 72(5), pp.2113-2119.

Boboc, A. (2020). Evaluation of bacterial ligands involved in receptor-mediated phagocytosis in *Tetrahymena pyriformis*. *MRes thesis*, Lancaster University.

Boenigk, J., Matz, C., Jürgens, K. and Arndt, H. (2001). The influence of preculture conditions and food quality on the ingestion and digestion process of three species of heterotrophic nanoflagellates. *Microbial Ecology*, 42(2), pp.168-176.

Borrelli, F., Romano, B., Petrosino, S., Pagano, E., Capasso, R., Coppola, D., Battista, G., Orlando, P., Di Marzo, V. and Izzo, A. (2014). Palmitoylethanolamide, a naturally occurring lipid, is an orally effective intestinal anti-inflammatory agent. *British Journal of Pharmacology*, 172(1), pp.142-158.

Boskovic, J., Arnold, J., Stilion, R., Gordon, S., Sim, R., Rivera-Calzada, A., Wienke, D. Isacke, C., Martinez-Pomares, L. and Llorca, O. (2006). Structural model for the mannose receptor family uncovered by electron microscopy of endo180 and the mannose receptor. *Journal of Biological Chemistry*, 281(13), pp.8780-8787.

Bracha, R., Kobiler, D. and Mirelman, D. (1982). Attachment and ingestion of bacteria by trophozoites of *Entamoeba histolytica*. *Infection and immunity*, 36(1), pp.396–406.

Brenner, S. and Miller, J., (2002). *Encyclopedia Of Genetics. Vol 1*. San Diego: Academic Press.

Bryant, D. (1982). Phycoerythrocyanin and phycoerythrin: properties and occurrence in cyanobacteria. *Microbiology*, 128(4), pp.835-844.

Cambi, A., Koopman, M. and Figdor, C. (2005). How C-type lectins detect pathogens. *Cellular Microbiology*, 7(4), pp.481-488.

Capriulo, G. and Degnan, C. (1991). Effect of food concentration on digestion and vacuole passage time in the heterotrichous marine ciliate *Fibrea salina*. *Marine Biology*, 110(2), pp.199-202.

Caron DA and Goldman JC. (1990) Nutrient regeneration. In: Capriulo GM (ed) The ecology of marine protozoa. *Oxford university Press, New York*. pp.283–306.

Castellano, C., Cabib, S., Palmisano, A., Di Marzo, V. and Puglisi-Allegra, S. (1997). The effects of anandamide on memory consolidation in mice involve both D1and D2 dopamine receptors. *Behavioural Pharmacology*, 8(8), pp.707-712.

Caterina, M., Schumacher, M., Tominaga, M., Rosen, T., Levine, J. and Julius, D. (1997). The capsaicin receptor: a heat-activated ion channel in the pain pathway. *Nature*, 389(6653), pp.816-824.

Chua, R. and Wong, S. (2013). SNX3 recruits to phagosomes and negatively regulates phagocytosis in dendritic cells. *Immunology*, 139(1), pp.30-47.

Cohen, I., Gerrard, J. and White, J. (1982). Ultrastructure of clots during isometric contraction. *The Journal of Cell Biology*, 93(3), pp.775-787.

Corliss, J.O. (2002). Biodiversity and biocomplexity of the Protists and an overview of their significant roles in maintenance of our biosphere. *Acta Protozoologica*, 41(3), pp.199–219.

Cravatt, B., Giang, D., Mayfield, S., Boger, D., Lerner, R. and Gilula, N. (1996). Molecular characterization of an enzyme that degrades neuromodulatory fatty-acid amides. *Nature*, 384(6604), pp.83-87.

Cui, Y., Oh, Y., Lim, J., Youn, M., Lee, I., Pak, H., Park, W., Jo, W. and Park, S. (2012). AFM study of the differential inhibitory effects of the green tea polyphenol (−)-epigallocatechin-3-gallate (EGCG) against Gram-positive and Gram-negative bacteria. *Food Microbiology*, 29(1), pp.80-87.

Damiani, M., Pavarotti, M., Leiva, N., Lindsay, A., McCaffrey, M. and Colombo, M. (2004). Rab coupling protein associates with phagosomes and regulates recycling from the phagosomal compartment. *Traffic*, 5(10), pp.785-797.

De Matos Feijó, F., Bertoluci, M. and Reis, C. (2011). Serotonin and hypothalamic control of hunger: a review. *Revista da Associação Médica Brasileira (English Edition)*, 57(1), pp.74-77.

De Petrocellis, L. and Di Marzo, V. (2005). Lipids as regulators of the activity of transient receptor potential type V1 (TRPV1) channels. *Life Sciences*, 77(14), pp.1651-1666.

Deutsch, D. (2016). A personal retrospective: elevating anandamide (AEA) by targeting fatty acid amide hydrolase (FAAH) and the fatty acid binding proteins (FABPs). *Frontiers in Pharmacology*, 7(370), pp.1-4.

Deutsch, D. and Chin, S. (1993). Enzymatic synthesis and degradation of anandamide, a cannabinoid receptor agonist. *Biochemical Pharmacology*, 46(5), pp.791-796

Devane, W., Hanus, L., Breuer, A., Pertwee, R., Stevenson, L., Griffin, G., Gibson, D., Mandelbaum, A., Etinger, A. and Mechoulam, R. (1992). Isolation and structure of a brain constituent that binds to the cannabinoid receptor. *Science*, 258(5090), pp.1946-1949.

Devinsky, O., Cilio, M., Cross, H., Fernandez-Ruiz, J., French, J., Hill, C., Katz, R., Di Marzo, V., Jutras-Aswad, D., Notcutt, W., Martinez-Orgado, J., Robson, P., Rohrback, B., Thiele, E., Whalley, B. and Friedman, D. (2014). Cannabidiol: pharmacology and potential therapeutic role in epilepsy and other neuropsychiatric disorders. *Epilepsia*, 55(6), pp.791-802.

Dey, R., Pernin, P. and Bodennec, J. (2010). Endocannabinoids inhibit the growth of free-living amoebae. *Antimicrobial Agents and Chemotherapy*, 54(7), pp.3065-3067.

Di Marzo, V. and De Petrocellis, L. (2012). Why do cannabinoid receptors have more than one endogenous ligand? *Philosophical Transactions of the Royal Society B: Biological Sciences*, 367(1607), pp.3216-3228.

Di Marzo, V., Melck, D., Bisogno, T. and De Petrocellis, L. (1998). Endocannabinoids: endogenous cannabinoid receptor ligands with neuromodulatory action. *Trends in Neurosciences*, 21(12), pp.521-528.

Di Marzo, V., Fontana, A., Cadas, H., Schinelli, S., Cimino, G., Schwartz, J. and Piomelli, D. (1994). Formation and inactivation of endogenous cannabinoid anandamide in central neurons. *Nature*, 372(6507), pp.686-691.

Dinh, T., Kathuria, S. and Piomelli, D. (2004). RNA interference suggests a primary role for monoacylglycerol lipase in the degradation of the endocannabinoid 2-arachidonoylglycerol. *Molecular Pharmacology*, 66(5), pp.1260-1264.

Dinh, T., Carpenter, D., Leslie, F., Freund, T., Katona, I., Sensi, S., Kathuria, S. and Piomelli, D. (2002). Brain monoglyceride lipase participating in endocannabinoid inactivation. *Proceedings of the National Academy of Sciences*, 99(16), pp.10819-10824.

Dinh, T., Freund, T. and Piomelli, D. (2002). A role for monoglyceride lipase in 2-arachidonoylglycerol inactivation. *Chemistry and Physics of Lipids*, 121(1-2), pp.149-158.

Drickamer, K. and Fadden, A. (2002). Genomic analysis of C-type lectins. *Biochemical Society Symposia*, 69(4), pp.59-72.

Duclos, S. (2003). Remodeling of endosomes during lysosome biogenesis involves `kiss and run' fusion events regulated by rab5. *Journal of Cell Science*, 116(5), pp.907-918.

Dunne, D.W., Resnick, D., Greenberg, J., Krieger, M. and Joiner, K.A. (1994). The type I macrophage scavenger receptor binds to gram-positive bacteria and recognizes lipoteichoic acid. *Proceedings of the National Academy of Sciences*, 91(5), pp.1863–1867.

Dürichen, H., Siegmund, L., Burmester, A., Fischer, M.S. and Wöstemeyer, J. (2016). Ingestion and digestion studies in *Tetrahymena pyriformis* based on chemically modified microparticles. *European Journal of Protistology*, 52(1), pp.45–57.

East, L. and Isacke, C.M. (2002). The mannose receptor family. *Biochimica et Biophysica Acta (BBA) - General Subjects*, 1572(2–3), pp.364–386.

Epps, D., Schmid, P., Natarajan, V. and Schmid, H. (1979). N-acylethanolamine accumulation in infarcted myocardium. *Biochemical and Biophysical Research Communications*, 90(2), pp.628-633.

Everroad, R. and Wood, A. (2012). Phycoerythrin evolution and diversification of spectral phenotype in marine *Synechococcus* and related picocyanobacteria. *Molecular Phylogenetics and Evolution*, 64(3), pp.381-392.

Fenchel, T. (1987). Ecology of protozoa: the biology of free-living phagotrophic protists. *New York: Springer series in Contemporary Bioscience.*

Fernández-Ruiz, J., Moreno-Martet, M., Rodríguez-Cueto, C., Palomo-Garo, C., Gómez-Cañas, M., Valdeolivas, S., Guaza, C., Romero, J., Guzmán, M., Mechoulam, R. and Ramos, J. (2011). Prospects for cannabinoid therapies in basal ganglia disorders. *British Journal of Pharmacology*, 163(7), pp.1365-1378.

Ficner, R. and Huber, R. (1993). Refined crystal structure of phycoerythrin from *Porphyridium cruentum* at 0.23-nm resolution and localization of the gamma subunit. *European Journal of Biochemistry*, 218(1), pp.103-106.

Foissner, W. (2008). *Protist diversity and geographical distribution*. Dordrecht: Springer.

Fok, A., Lee, Y. and Allen, R. (1982). The correlation of digestive vacuole pH and size with the digestive cycle in *Paramecium caudatum 1*. *The Journal of Protozoology*, 29(3), pp.409-414.

Fu, J., Gaetani, S., Oveisi, F., Lo Verme, J., Serrano, A., Rodríguez de Fonseca, F., Rosengarth, A., Luecke, H., Di Giacomo, B., Tarzia, G. and Piomelli, D. (2003). Oleylethanolamide regulates feeding and body weight through activation of the nuclear receptor PPAR-α. *Nature*, 425(6953), pp.90-93.

Gaitán, A., Wood, J., Zhang, F., Makriyannis, A. and Lammi-Keefe, C. (2018). Endocannabinoid metabolome characterization of transitional and mature human milk. *Nutrients*, 10(9), p.1294.

Giang, D. and Cravatt, B. (1997). Molecular characterization of human and mouse fatty acid amide hydrolases. *Proceedings of the National Academy of Sciences*, 94(6), pp.2238-2242

Gomez del Pulgar, T., Velasco, G. and Guzman, M. (2000). The CB1 cannabinoid receptor is coupled to the activation of protein kinase B/Akt. *Biochemical Journal*, 347(2), pp.369-373.

Granja, A., Carrillo-Salinas, F., Pagani, A., Gómez-Cañas, M., Negri, R., Navarrete, C., Mecha, M., Mestre, L., Fiebich, B., Cantarero, I., Calzado, M., Bellido, M., Fernandez-Ruiz, J., Appendino, G., Grinspoon, L. and Bakalar, J. (1997). *Marihuana, the forbidden medicine*. *Revised Edition.* New Haven, Yale University Press.

Gupta, A. and Gupta, G. (2012). C-Type Lectins Family. *Animal Lectins: Form, Function and Clinical Applications*, 22(1) pp.473-482.

Habayeb, O., Bell, S. and Konje, J. (2002). Endogenous cannabinoids: metabolism and their role in reproduction. *Life Sciences*, 70(17), pp.1963-1977.

Hampton, R., Golenbock, D., Penman, M., Krieger, M. and Raetz, C. (1991). Recognition and plasma clearance of endotoxin by scavenger receptors. *Nature*, 352(6333), pp.342-344.

Harb, O.S., Venkataraman, C., Haack, B.J., Gao, L.Y. and Abu Kwaik, Y. (1998). Heterogeneity in the attachment and uptake mechanisms of the Legionnaires' disease bacterium, *Legionella pneumophila*, by protozoan hosts. *Applied and Environmental Microbiology*, 64(1), pp.126–132.

Harrison, R., Bucci, C., Vieira, O., Schroer, T. and Grinstein, S. (2003). Phagosomes fuse with late endosomes and/or lysosomes by extension of membrane protrusions along microtubules: Role of Rab7 and RILP. *Molecular and Cellular Biology*, 23(18), pp.6494-6506.

Hind, W., Tufarelli, C., Neophytou, M., Anderson, S., England, T. and O'Sullivan, S. (2015). Endocannabinoids modulate human blood-brain barrier permeabilityin vitro. *British Journal of Pharmacology*, 172(12), pp.3015-3027.

Howlett, A. (1998). The CB1 cannabinoid receptor in the brain. *Neurobiology of Disease*, 5(6), pp.405-416.

Howlett, A. and Mukhopadhyay, S. (2000). Cellular signal transduction by anandamide and 2-arachidonoylglycerol. *Chemistry and Physics of Lipids*, 108(1-2), pp.53-70.

Howlett, A., Barth, F., Bonner, T., Cabral, G., Casellas, P., Devane, W., Felder, C., Herkenham, M., Mackie, K., Martin, B., Mechoulam, R. and Pertwee, R. (2002). International union of pharmacology. XXVII. Classification of cannabinoid receptors. *Pharmacological Reviews*, 54(2), pp.161-202.

Huynh, K., Eskelinen, E., Scott, C., Malevanets, A., Saftig, P. and Grinstein, S. (2007). LAMP proteins are required for fusion of lysosomes with phagosomes. *The EMBO Journal*, 26(2), pp.313-324.

Iannotti, F., Di Marzo, V. and Petrosino, S. (2016). Endocannabinoids and endocannabinoid-related mediators: Targets, metabolism and role in neurological disorders. *Progress in Lipid Research*, 62(1), pp.107-128.

Iannotti, F., Hill, C., Leo, A., Alhusaini, A., Soubrane, C., Mazzarella, E., Russo, E., Whalley, B., Di Marzo, V. and Stephens, G. (2014). Nonpsychotropic plant cannabinoids, cannabidivarin (CBDV) and cannabidiol (CBD), activate and desensitize transient receptor potential vanilloid 1 (TRPV1) channels in vitro: potential for the treatment of neuronal hyperexcitability. *ACS Chemical Neuroscience*, 5(11), pp.1131-1141.

Iffland, K. and Grotenhermen, F. (2017). An update on safety and side effects of cannabidiol: A review of clinical data and relevant animal studies. *Cannabis and Cannabinoid Research*, 2(1), pp.139-154.

Iversen, L. (2000). *The Science of Marijuana*. Oxford, UK: Oxford University Press.

Izzo, A. (2001). The gastrointestinal pharmacology of cannabinoids. *Current Opinion in Pharmacology*, 1(6), pp.597-603.

Jacobson, D. and Anderson, D. (1996). Widespread phagocytosis of ciliates and other protists by marine mixotrophic and heterotrophic thecate dinoflagellates. *Journal of Phycology*, 32(2), pp.279-285.

Janeway, C.A. and Medzhitov, R. (2002). Innate immune recognition. *Annual Review of Immunology*, 20(1), pp.197–216.

Jeffreys, L., Girvan, H., McLean, K. and Munro, A. (2018). Characterization of cytochrome P450 enzymes and their applications in synthetic biology. *Methods in Enzymology*, 608(1), pp.189-261.

Jones, A. (2017). Investigation of the effects of cannabinoids on feeding behaviour in the free living ciliate *Tetrahymena pyriformis*. *Dissertation, MSci Biomedicine*, Lancaster University.

Johansson, M., Lehto, M., Tanhuanpää, K., Cover, T. and Olkkonen, V. (2005). The oxysterol-binding protein homologue ORP1L interacts with Rab7 and alters functional properties of late endocytic compartments. *Molecular Biology of the Cell*, 16(12), pp.5480-5492.

Jonsson, P. (1986). Particle size selection, feeding rates and growth dynamics of marine planktonic oligotrichous ciliates (Ciliophora: Oligotrichina). *Marine Ecology Progress Series*, 33(3), pp.265-277.

Karava, V., Fasia, L. and Siafaka-Kapadai, A. (2001). Anandamide amidohydrolase activity, released in the medium by *Tetrahymena pyriformis*. Identification and partial characterization. *FEBS Letters*, 508(3), pp.327-331.

Karava, V., Zafiriou, P., Fasia, L., Anagnostopoulos, D., Boutou, E., Vorgias, C., Maccarrone, M. and Siafaka-Kapadai, A. (2005). Anandamide metabolism by *Tetrahymena pyriformis* in vitro. Characterization and identification of a 66 kDa fatty acid amidohydrolase. *Biochimie*, 87(11), pp.967-974.

Kathol, M., Norf, H., Arndt, H. and Weitere, M. (2009). Effects of temperature increase on the grazing of planktonic bacteria by biofilm-dwelling consumers. *Aquatic Microbial Ecology*, 55(1), pp.65-79.

Kendall, D. and Yudowski, G. (2017). Cannabinoid receptors in the central nervous system: their signaling and Roles in Disease. *Frontiers in Cellular Neuroscience*, 10(294), pp.1-6.

Kerrigan, A. and Brown, G. (2009). C-type lectins and phagocytosis. *Immunobiology*, 214(7), pp.562-575.

Kleberg, K., Hassing, H. and Hansen, H. (2014). Classical endocannabinoid-like compounds and their regulation by nutrients. *BioFactors*, 40(4), pp.363-372.

Klein, T. (2005). Cannabinoid-based drugs as anti-inflammatory therapeutics. *Nature Reviews Immunology*, 5(5), pp.400-411.

Konrad, R., Major, C. and Wolf, B. (1994). Diacylglycerol hydrolysis to arachidonic acid Is necessary for insulin secretion from isolated pancreatic islets: sequential actions of diacylglycerol and monoacylglycerol lipases. *Biochemistry*, 33(45), pp.13284-13294.

Kozak, K., Gupta, R., Moody, J., Ji, C., Boeglin, W., DuBois, R., Brash, A. and Marnett, L. (2002). 15-Lipoxygenase metabolism of 2-arachidonylglycerol. *Journal of Biological Chemistry*, 277(26), pp.23278-23286.

Lambert, D. and Fowler, C. (2005). The endocannabinoid system: drug targets, lead compounds, and potential therapeutic applications. *ChemInform*, 36(45), pp.5059-5087.

Lanzoni, O., Fokin, S., Lebedeva, N., Migunova, A., Petroni, G. and Potekhin, A. (2016). Rare freshwater ciliate *Paramecium chlorelligerum* Kahl, 1935 and its macronuclear symbiotic bacterium "*Candidatus Holospora parva*". *Plos one*, 11(12), pp.167-928.

Lawe, D., Chawla, A., Merithew, E., Dumas, J., Carrington, W., Fogarty, K., Lifshitz, L., Tuft, R., Lambright, D. and Corvera, S. (2001). Sequential roles for phosphatidylinositol 3-phosphate and Rab5 in tethering and fusion of early endosomes via their interaction with EEA1. *Journal of Biological Chemistry*, 277(10), pp.8611-8617.

Leopoldo, M., Lacivita, E., Berardi, F., Perrone, R. and Hedlund, P. (2011). Serotonin 5-HT7 receptor agents: Structure-activity relationships and potential therapeutic applications in central nervous system disorders. *Pharmacology & Therapeutics*, 129(2), pp.120-148.

Levin, R., Grinstein, S. and Canton, J. (2016). The life cycle of phagosomes: formation, maturation, and resolution. *Immunological Reviews*, 273(1), pp.156-179.

Leweke, F., Piomelli, D., Pahlisch, F., Muhl, D., Gerth, C., Hoyer, C., Klosterkötter, J., Hellmich, M. and Koethe, D. (2012). Cannabidiol enhances anandamide signaling and alleviates psychotic symptoms of schizophrenia. *Translational Psychiatry*, 2(3), pp.94-94.

Liedtke, M., Heller, S. and Liedtke, W. (2010). TRP ion channel function in sensory transduction and cellular signalling cascades. Boca Raton (FL): CRC Press/Taylor & Francis; 2007. Contributors.

Lone, T. and Lone, R. (2012). Extraction of cannabinoids from *Cannabis sativa* L plant and its potential antimicrobial activity. *Universal Journal of Medicine and Dentistry*, 1(4), pp.51-55.

LoVerme, J., La Rana, G., Russo, R., Calignano, A. and Piomelli, D. (2005). The search for the palmitoylethanolamide receptor. *Life Sciences*, 77(14), pp.1685-1698.

Lu, H. and Mackie, K. (2016). An introduction to the endogenous cannabinoid system. *Biological Psychiatry*, 79(7), pp.516-525.

Luzio, J., Rous, B., Bright, N., Pryor, P., Mullock, B. and Piper, R. (2000). Lysosome-endosome fusion and lysosome biogenesis. *Journal of Cell Science*, 113(9), pp.1515-24.

Luzio, J., Gray, S. and Bright, N. (2010). Endosome–lysosome fusion: *Biochemical Society Transactions*, 38(6), pp.1413-1416.

Lynch, T. and Price, A. (2007). The effect of cytochrome P450 metabolism on drug response, interactions, and adverse effects. *American family physician*, 76(3), pp.391-396.

Maccarrone, M., Bab, I., Bíró, T., Cabral, G., Dey, S., Di Marzo, V., Konje, J., Kunos, G., Mechoulam, R., Pacher, P., Sharkey, K. and Zimmer, A. (2015). Endocannabinoid signalling at the periphery: 50 years after THC. *Trends in Pharmacological Sciences*, 36(5), pp.277-296.

Maccarrone, M., van der Stelt, M., Rossi, A., Veldink, G., Vliegenthart, J. and Agrò, A. (1998). Anandamide hydrolysis by human cells in culture and crain. *Journal of Biological Chemistry*, 273(48), pp.32332-32339.

Mackie, K. (2006). Mechanisms of CB1 receptor signalling: endocannabinoid modulation of synaptic strength. *International Journal of Obesity*, 30(1), pp. S19-S23.

Mackie, K. (2008). Cannabinoid receptors: where they are and what they do. *Journal of Neuroendocrinology*, 20(s1), pp.10-14.

McPartland, J. and Pruitt, P. (2002). Sourcing the code: searching for the evolutionary origins of cannabinoid receptors, vanilloid receptors, and anandamide. *Journal of Cannabis Therapeutics*, 2(1), pp.73-103.

McPartland, J., Matias, I., Di Marzo, V. and Glass, M. (2006). Evolutionary origins of the endocannabinoid system. *Gene*, 370(1), pp.64-74.

Mkpenie, V., Essien, E. and Udoh, I. (2012). Effect of extraction conditions on total polyphenol contents, antioxidant and antimicrobial activities of *Cannabis sativa* L. *Electronic Journal of Environmental, Agricultural and Food Chemistry,* 11(4), pp.300-307.

Mallet, P. and Beninger, R. (1996). The endogenous cannabinoid receptor agonist anandamide impairs memory in rats. *Behavioural Pharmacology*, 7(3), pp.276- 284.

Marie-Anaïs, F., Mazzolini, J., Herit, F. and Niedergang, F. (2016). Dynamin-actin cross talk contributes to phagosome formation and closure. Traffic, 17(5), pp.487–499.

Maroon, J. and Bost, J. (2018). Review of the neurological benefits of phytocannabinoids. *Surgical Neurology International*, 9(1), p.91.

Marzo, V., Bifulco, M. and Petrocellis, L. (2004). The endocannabinoid system and its therapeutic exploitation. *Nature Reviews Drug Discovery*, 3(9), pp.771-784.

Marzo, V. and Petrocellis, L. (2010). Endocannabinoids as regulators of transient receptor potential (TRP) channels: a further opportunity to develop new endocannabinoid-based therapeutic drugs. *Current Medicinal Chemistry*, 17(14), pp.1430-1449.

Matias, I., Bisogno, T., Melck, D., Vandenbulcke, F., Verger-Bocquet, M., De Petrocellis, L., Sergheraert, C., Breton, C., Di Marzo, V. and Salzet, M. (2001). Evidence for an

endocannabinoid system in the central nervous system of the leech Hirudo medicinalis. *Molecular Brain Research*, 87(2), pp.145-159.

McClean, D. and Zimmerman, A. (1976). Action of Δ^9-tetrahydrocannabinol on cell division and macromolecular synthesis in division-synchronized protozoa. *Pharmacology*, 14(4), pp. 307-321.

Mechoulam, R. (1986). The pharmacohistory of cannabis sativa, in cannabis as therapeutic agent. Boca Raton FL, USA: CRC Press.

Mechoulam, R., Ben-Shabat, S., Hanus, L., Ligumsky, M., Kaminski, N., Schatz, A., Gopher, A., Almog, S., Martin, B., Compton, D., Pertwee, R., Griffin, G., Bayewitch, M., Barg, J. and Vogel, Z. (1995). Identification of an endogenous 2-monoglyceride, present in canine gut, that binds to cannabinoid receptors. *Biochemical Pharmacology*, 50(1), pp.83-90.

Mechoulam, R. (2005). Plant cannabinoids: a neglected pharmacological treasure trove. *British Journal of Pharmacology*, 146(7), pp.913-915.

Méténier, G. (1984). Actin in *Tetrahymena paravorax*: ultrastructural localization of HMM-binding filaments in glycerinated cells1,2. *The Journal of Protozoology*, 31(2), pp.205-215.

Mitra, A., Flynn, K.J., Tillmann, U., Raven, J.A., Caron, D., Stoecker, D.K., Not, F., Hansen, P.J., Hallegraeff, G., Sanders, R., Wilken, S., McManus, G., Johnson, M., Pitta, P., Våge, S., Berge, T., Calbet, A., Thingstad, F., Jeong, H.J., Burkholder, J., Glibert, P.M., Granéli, E. and Lundgren, V. (2016). Defining planktonic protist functional groups on mechanisms for energy and nutrient acquisition: incorporation of diverse mixotrophic strategies. *Protist*, 167(2), pp.106–120.

Muller, W. (1980a). The membrane proteins of the vacuolar system I. Analysis of a novel method of intralysosomal iodination. *The Journal of Cell Biology*, 86(1), pp.292-303.

Muller, W. (1980b). The membrane proteins of the vacuolar system. II. Bidirectional flow between secondary lysosomes and plasma membrane. *The Journal of Cell Biology*, 86(1), pp.304-314.

Natarajan, V., Reddy, P., Schmid, P. and Schmid, H. (1981). On the biosynthesis and metabolism of N-acylethanolamine phospholipids in infarcted dog heart. *Biochimica et Biophysica Acta (BBA) - Lipids and Lipid Metabolism*, 664(2), pp.445-448.

Navarrete, M. and Araque, A. (2010). Endocannabinoids potentiate synaptic transmission through stimulation of astrocytes. *Neuron*, 68(1), pp.113-126.

Nohynek, L., Alakomi, H., Kähkönen, M., Heinonen, M., Helander, I., Oksman-Caldentey, K. and Puupponen-Pimiä, R. (2006). Berry phenolics: antimicrobial properties and mechanisms of action against severe human pathogens. *Nutrition and Cancer*, 54(1), pp.18-32.

Nordmann, M., Cabrera, M., Perz, A., Bröcker, C., Ostrowicz, C., Engelbrecht-Vandré, S. and Ungermann, C. (2010). The Mon1-Ccz1 complex Is the GEF of the late endosomal Rab7 homolog Ypt7. *Current Biology*, 20(18), pp.1654-1659.

O'Sullivan, S., Kendall, D. and Randall, M. (2009). Time-dependent vascular effects of endocannabinoids mediated by peroxisome proliferator-activated receptor gamma (PPAR). *PPAR Research 2009(1),* pp.1-9.

O'Sullivan, S., Tarling, E., Bennett, A., Kendall, D. and Randall, M. (2005). Novel time-dependent vascular actions of Δ9-tetrahydrocannabinol mediated by peroxisome proliferator-activated receptor gamma. *Biochemical and Biophysical Research Communications*, 337(3), pp.824-831.

Pacher, P. (2006). The endocannabinoid system as an emerging target of pharmacotherapy. *Pharmacological Reviews*, 58(3), pp.389-462.

Palazuelos, J., Aguado, T., Pazos, M., Julien, B., Carrasco, C., Resel, E., Sagredo, O., Benito, C., Romero, J., Azcoitia, I., Fernández-Ruiz, J., Guzmán, M. and Galve-Roperh, I. (2009). Microglial CB2 cannabinoid receptors are neuroprotective in Huntington's disease excitotoxicity. *Brain*, 132(11), pp.3152-3164.

Parry, J. (2004). Protozoan grazing of freshwater biofilms. *Advances in Applied Microbiology*, 54(1), pp.167-196.

Pauwels, A., Trost, M., Beyaert, R. and Hoffmann, E. (2017). Patterns, receptors, and signals: regulation of phagosome maturation. *Trends in Immunology*, 38(6), pp.407-422.

Perkins, F., Haas, L., Phillips, D. and Webb, K. (1981). Ultrastructure of a marine *Synechococcus* possessing spinae. *Canadian Journal of Microbiology*, 27(3), pp.318-329.

Peplowska, K., Markgraf, D., Ostrowicz, C., Bange, G. and Ungermann, C. (2007). The CORVET tethering complex interacts with the yeast Rab5 homolog Vps21 and Is Involved in endo-lysosomal biogenesis. *Developmental Cell*, 12(5), pp.739-750.

Pertwee, R. (1997). Pharmacology of cannabinoid CB1 and CB2 receptors. *Pharmacology & Therapeutics*, 74(2), pp.129-180.

Pertwee, R. (2015). *Handbook of cannabis*. The Oxford Press, pp.157-162.

Peruń, A., Biedroń, R., Konopiński, M.K., Białecka, A., Marcinkiewicz, J. and Józefowski, S. (2016). Phagocytosis of live versus killed or fluorescently labeled bacteria by macrophages differ in both magnitude and receptor specificity. *Immunology and Cell Biology*, 95(5), pp.424–435.

Plattner, H. (2010). Membrane trafficking in protozoa. *International Review of Cell and Molecular Biology*, 280(1) pp.79-184.

Poirier, V. and Av-gay, Y. (2015). Intracellular growth of bacterial pathogens: The role of secreted effector proteins in the control of phagocytosed microorganisms. *Virulence Mechanisms of Bacterial Pathogens, Fifth Edition*, ed. Kudva, I., Cornick, N. and Plummer, P. Washington: ASM Press.pp.693-713.

Prescott, S. and Majerus, P. (1983). Characterization of 1,2-diacylglycerol hydrolysis in human platelets. Demonstration of an arachidonoyl-monoacylglycerol intermediate. *Journal of Biology Chem.*, 258(2), pp.764-769.

Pringle, H., Bradley, S. and Harris, L. (1979). Susceptibility of *Naegleria fowleri* to delta 9-tetrahydrocannabinol. *Antimicrobial Agents and Chemotherapy*, 16(5), pp.674-679.

Ramirez, B. (2005). Prevention of Alzheimer's disease pathology by cannabinoids: neuroprotection mediated by blockade of microglial activation. *Journal of Neuroscience*, 25(8), pp.1904-1913.

Ramirez, S., Hasko, J., Skuba, A., Fan, S., Dykstra, H., McCormick, R., Reichenbach, N., Krizbai, I., Mahadevan, A., Zhang, M., Tuma, R., Son, Y. and Persidsky, Y. (2012). Activation of cannabinoid receptor 2 attenuates leukocyte-endothelial cell interactions and blood-brain barrier dysfunction under inflammatory conditions. *Journal of Neuroscience*, 32(12), pp.4004-4016.

Ramoino, P., Fronte, P., Fato, M., Beltrame, F., Robello, M. and Diaspro, A. (2001). Fluid phase and receptor-mediated endocytosis in *Paramecium primaurelia* by fluorescence confocal laser scanning microscopy. *European Biophysics Journal*, 30(5), pp.305-312.

Ricketts, T. and Rappitt, A. (1976). Endocytosis, digestive vacuolar movement and exocytosis on refeeding starved *Tetrahymena pyriformis* GL-9. *Protoplasma*, 87(1-3), pp.221-236.

Ricketts, T. (1979). Temporal movement of digestive vacuoles in fed *Tetrahymena pyriformis* GL-9. *Protoplasma*, 100(3-4), pp.317-322.

Ricketts, T. (1983). Dichloroisoproterenol and digestive vacuolar formation, movement and egestion in *Tetrahymena pyriformis* GL-9. *Protoplasma*, 115(1), pp.25-33.

Roberts, C., Jager, G., Christiansen, P. and Kirkham, T. (2019). Exploring the munchies: An online survey of users' experiences of cannabis effects on appetite and the development of a Cannabinoid Eating Experience Questionnaire. *Journal of Psychopharmacology*, 33(9), pp.1149-1159.

Roberts, E., Zubkov, M., Martin-Cereceda, M., Novarino, G. and Wootton, E. (2006). Cell surface lectin-binding glycoconjugates on marine planktonic protists. *FEMS Microbiology Letters*, 265(2), pp.202-207.

Romano, M. and Lograno, M. (2012). Involvement of the peroxisome proliferator-activated receptor (PPAR) alpha in vascular response of endocannabinoids in the bovine ophthalmic artery. *European Journal of Pharmacology*, 683(1-3), pp.197-203.

Rothstein, T. (1974). Lysosomal physiology in *Tetrahymena*: III. Pharmacological studies on acid hydrolase release and the ingestion and egestion of dimethylbenzanthracene particles. *The Journal of Cell Biology*, 62(3), pp.844-859.

Sang, N., Zhang, J. and Chen, C. (2006). PGE2glycerol ester, a COX-2 oxidative metabolite of 2-arachidonoyl glycerol, modulates inhibitory synaptic transmission in mouse hippocampal neurons. *The Journal of Physiology*, 572(3), pp.735-745.

Sagredo, O., García-Arencibia, M., de Lago, E., Finetti, S., Decio, A. and Fernández-Ruiz, J. (2007). Cannabinoids and neuroprotection in basal ganglia disorders. *Molecular Neurobiology*, 36(1), pp.82-91.

Sanchez, M. (2003). Activation of phosphoinositide 3-kinase/PKB pathway by CB1 and CB2 cannabinoid receptors expressed in prostate PC-3 cells. Involvement in Raf-1 stimulation and NGF induction. *Cellular Signalling*, 15(9), pp.851-859.

Satir, B. (1989). Signal transduction events associated with exocytosis in ciliates. *The Journal of Protozoology*, 36(4), pp.382-389.

Sattler, N., Bosmani, C., Bärisch, C., Guého, A., Gopaldass, N., Dias, M., Leuba, F., Bruckert, F., Cosson, P. and Soldati, T. (2018). Functions of the *Dictyostelium* LIMP-2 and CD36 homologues in bacteria uptake, phagolysosome biogenesis and host cell defense. *Journal of Cell Science*, 131(17),

Savina, A., Jancic, C., Hugues, S., Guermonprez, P., Vargas, P., Moura, I., Lennon-Duménil, A., Seabra, M., Raposo, G. and Amigorena, S. (2006). NOX2 controls phagosomal pH to regulate antigen processing during cross-presentation by dendritic cells. *Cell*, 126(1), pp.205-218.

Schmid, P., Paria, B., Krebsbach, R., Schmid, H. and Dey, S. (1997). Changes in anandamide levels in mouse uterus are associated with uterine receptivity for embryo implantation. *Proceedings of the National Academy of Sciences*, 94(8), pp.4188-4192.

Schmid, P., Reddy, P., Natarajan, V. and Schmid, H. (1983). Metabolism of N-acylethanolamine phospholipids by a mammalian phosphodiesterase of the phospholipase D type. *Journal of Biological Chemistry*, 258(15), pp.9302-6.

Schmid, H., Schmid, P. and Zuzarte-Augustin, M. (1985). Properties of rat liver N-acylethanolamine amidohydrolase *Journal of Biological Chemistry*, 260(26), pp.14145-9.

Seeman, P. (2016). Cannabidiol is a partial agonist at dopamine D2High receptors, predicting its antipsychotic clinical dose. *Translational Psychiatry*, 6(10), pp.920-e920.

Simpson, C., Itabe, H., Reynolds, C., King, W. and Glomset, J. (1991). Swiss 3T3 cells preferentially incorporate sn-2-arachidonoyl monoacylglycerol into sn-1-stearoyl-2-arachidonoyl phosphatidylinositol. *Journal of Biological Chemistry.*, 266(4), pp.15902-15909.

Six, C., Thomas, J., Garczarek, L., Ostrowski, M., Dufresne, A., Blot, N., Scanlan, D. and Partensky, F. (2007). Diversity and evolution of phycobilisomes in marine *Synechococcus* spp.: a comparative genomics study. *Genome Biology*, 8(12), p.R259.

Soria-Gómez, E., Bellocchio, L., Reguero, L., Lepousez, G., Martin, C., Bendahmane, M., Ruehle, S., Remmers, F., Desprez, T., Matias, I., Wiesner, T., Cannich, A., Nissant, A., Wadleigh, A., Pape, H., Chiarlone, A., Quarta, C., Verrier, D., Vincent, P., Massa, F., Lutz, B., Guzmán, M., Gurden, H., Ferreira, G., Lledo, P., Grandes, P. and Marsicano, G. (2014). The endocannabinoid system controls food intake via olfactory processes. *Nature Neuroscience*, 17(3), pp.407-415.

Šrejber, M., Navrátilová, V., Paloncýová, M., Bazgier, V., Berka, K., Anzenbacher, P. and Otyepka, M. (2018). Membrane-attached mammalian cytochromes P450: An overview of the membrane's effects on structure, drug binding, and interactions with redox partners. *Journal of Inorganic Biochemistry*, 183(1), pp.117-136.

Stahl, P.D. and Ezekowitz, R.A.B. (1998). The mannose receptor is a pattern recognition receptor involved in host defense. *Current Opinion in Immunology*, 10(1), pp.50–55.

Stella, N., Schweitzer, P. and Piomelli, D. (1997). A second endogenous cannabinoid that modulates long-term potentiation. *Nature*, 388(6644), pp.773-778.

Stella, N. (2010). Cannabinoid and cannabinoid-like receptors in microglia, astrocytes, and astrocytomas. *Glia*, 58(9), pp.1017-1030.

Stiedl, O., Pappa, E., Konradsson-Geuken, Ã. and Ã–gren, S. (2015). The role of the serotonin receptor subtypes 5-HT1A and 5-HT7 and its interaction in emotional learning and memory. *Frontiers in Pharmacology*, 6 (162), pp.1-17.

Stuart, L., Deng, J., Silver, J., Takahashi, K., Tseng, A., Hennessy, E., Ezekowitz, R. and Moore, K. (2005). Response to *Staphylococcus aureus* requires CD36-mediated phagocytosis triggered by the COOH-terminal cytoplasmic domain. *Journal of Cell Biology*, 170(3), pp.477-485.

Sun, Y., Alexander, S., Garle, M., Gibson, C., Hewitt, K., Murphy, S., Kendall, D. and Bennett, A. (2007). Cannabinoid activation of PPARα; a novel neuroprotective mechanism. *British Journal of Pharmacology*, 152(5), pp.734-743.

Swanson JA. (2008). Shaping cups into phagosomes and macropinosomes. *Nature Reviews Molecular Cell Biology*, 9(8), pp.639–649.

Taylor, B., Taylor, M., Dinter, T. and Bracher, A. (2013). Estimation of relative phycoerythrin concentrations from hyperspectral underwater radiance measurements--A statistical approach. *Journal of Geophysical Research: Oceans*, 118(6), pp.2948-2960.

Tiggemann, R. and Plattner, H. (1981). Localization of actin in the cortex of *Paramecium tetraurelia* cells by immuno- and affinity-fluorescence microscopy. *European Journal of Cell Biology*, 24(2), pp.184-90.

Tiggemann, R., Plattner, H., Rasched, I., Baeuerle, P. and Wachter, E. (1981). Quantitative data on peroxidatic markers for electron microscopy. With a note on actin identification in Paramecium cells. *Journal of Histochemistry & Cytochemistry*, 29(12), pp.1387-1396.

TGD- Homolog details for cyp1 (2019). *TGD | Homolog details for cyp1*. [online] Tetrahymena Genomics DataBase. Available at: http://ciliate.org/index.php/searchdetails/homologs/cyp1 [Accessed 22 Dec. 2019].

Thurman, J., Drinkall, J. and Parry, J. (2010). Digestion of bacteria by the freshwater ciliate *Tetrahymena pyriformis*. *Aquatic Microbial Ecology*, 60(2), pp.163-174.

Toth, M. (2003). 5-HT1A receptor knockout mouse as a genetic model of anxiety. *European Journal of Pharmacology*, 463(1-3), pp.177-184.

Turner, C.E. and Elsohly, M.A. (1981) Biological activity of cannabichromene, its homologs and isomers. *Journal of Clinical Pharmacology* 21(1), pp.283-291.

Turu, G. and Hunyady, L. (2009). Signal transduction of the CB1 cannabinoid receptor. *Journal of Molecular Endocrinology*, 44(2), pp.75-85.

Ujváry, I. and Hanuš, L. (2016). Human metabolites of cannabidiol: A review on their formation, biological activity, and relevance in therapy. *Cannabis and Cannabinoid Research*, 1(1), pp.90-101.

Van der Stelt, M., Trevisani, M., Vellani, V., De Petrocellis, L., Schiano Moriello, A., Campi, B., McNaughton, P., Geppetti, P. and Di Marzo, V. (2005). Anandamide acts as an intracellular messenger amplifying Ca^{2+} influx via TRPV1 channels. *The EMBO Journal*, 24(17), pp.3026-3037.

van Klingeren, B. and ten Ham, M. (1976). Antibacterial activity of Δ9-tetrahydrocannabinol and cannabidiol. *Antonie van Leeuwenhoek*, 42(1-2), pp.9-12.

Van Sickle, M. (2005). Identification and functional characterization of brainstem cannabinoid CB2 receptors. *Science*, 310(5746), pp.329-332.

Venkataraman, C., Haack, B.J., Bondada, S. and Kwaik, Y.A. (1997). Identification of a Gal/GalNAc lectin in the protozoan *Hartmannella vermiformis* as a potential receptor for attachment and invasion by the Legionnaires' disease bacterium. *The Journal of Experimental Medicine*, 186(4), pp.537–547.

Vieira, O., Botelho, R. and Grinstein, S., 2002. Phagosome maturation: aging gracefully. *Biochemical Journal*, 366(3), pp.689-704.

Vieira, O., Botelho, R., Rameh, L., Brachmann, S., Matsuo, T., Davidson, H., Schreiber, A., Backer, J., Cantley, L. and Grinstein, S. (2001). Distinct roles of class I and class III phosphatidylinositol 3-kinases in phagosome formation and maturation. *The Journal of Cell Biology*, 155(1), pp.19-26.

Viscomi, M., Oddi, S., Latini, L., Pasquariello, N., Florenzano, F., Bernardi, G., Molinari, M. and Maccarrone, M. (2009). Selective CB2 receptor agonism protects central neurons from remote axotomy-induced apoptosis through the PI3K/Akt Pathway. *Journal of Neuroscience*, 29(14), pp.4564-4570.

Vogel, G., Thilo, L., Schwarz, H. and Steinhart, R. (1980). Mechanism of phagocytosis in *Dictyostelium discoideum*: phagocytosis is mediated by different recognition sites as disclosed by mutants with altered phagocytotic properties. *Journal of Cell Biology*, 86(2), pp.456–465.

Waku, K. and Sugiura, T. (2003). 2-Arachidonoylglycerol, an endogenous cannabinoid receptor ligand in the nervous tissue. *Journal of Neurochemistry*, 85(2), pp.11-11

Wanlahbeh, N. (2020). An investigation into the targets for cannabinoid action in the ciliate *Tetrahymena pyriformis. MRes thesis, Lancaster University*.

Walter, L., Franklin, A., Witting, A., Wade, C., Xie, Y., Kunos, G., Mackie, K. and Stella, N. (2003). Nonpsychotropic cannabinoid receptors regulate microglial cell migration. *The Journal of Neuroscience*, 23(4), pp.1398-1405.

Whittaker, R. and Margulis, L. (1978). Protist classification and the kingdoms of organisms. *Biosystems*, 10(1-2), pp.3-18.

Whyte, L., Ryberg, E., Sims, N., Ridge, S., Mackie, K., Greasley, P., Ross, R. and Rogers, M. (2009). The putative cannabinoid receptor GPR55 affects osteoclast function in vitro and bone mass in vivo. *Proceedings of the National Academy of Sciences*, 106(38), pp.16511-16516.

Wilks, S.A. and Sleigh, M.A. (2004). Lectin binding sites on *Euplotes mutabilis* (Tuffrau, 1960) and the implications for food particle selection. *European Journal of Protistology*, 40(2), pp.153–162.

Witkowski, G., Rola, R. and Szulczyk, P. (2012). Effect of cyclic adenosine monophosphate on the G protein-dependent inward rectifier K(+)-like channel current in medial prefrontal cortex pyramidal neurons. *Journal of physiology and pharmacology 2012*, 63(5), pp.457-462.

Wollert, T. and Hurley, J. (2010). Molecular mechanism of multivesicular body biogenesis by ESCRT complexes. *Nature*, 464(7290), pp.864-869.

Wong, O. (2017). Investigation of prey ingestion and digestion in the ciliate predator *Tetrahymena pyriformis* and the impact on growth. *Masters Thesis- Lancaster University*.

Wootton, E., Zubkov, M., Jones, D., Jones, R., Martel, C., Thornton, C. and Roberts, E. (2007). Biochemical prey recognition by planktonic protozoa. *Environmental Microbiology*, 9(1), pp.216-222.

Xu, H., Zhang, W. and Jiang, Y. (2014). Do early colonization patterns of periphytic ciliate fauna reveal environmental quality status in coastal waters? *Environmental Science and Pollution Research*, 21(11), pp.7097-7112.

Yan, J. and Cai, Z. (2010). Molecular evolution and functional divergence of the cytochrome P450 3 (CYP3) family in actinopterygii (Ray-Finned Fish). *Plos one*, 5(12), p.14276.

Yates, R., Hermetter, A. and Russell, D. (2009). Recording phagosome maturation through the real-time, spectrofluorometric measurement of hydrolytic activities. *Macrophages and Dendritic Cells*, 531(1) pp.157-171.

Zani, I., Stephen, S., Mughal, N., Russell, D., Homer-Vanniasinkam, S., Wheatcroft, S. and Ponnambalam, S. (2015). Scavenger receptor structure and function in health and disease. *Cells*, 4(2), pp.178-201.

Zou, S. and Kumar, U. (2018). Cannabinoid receptors and the endocannabinoid system: signalling and function in the central nervous system. *International Journal of Molecular Sciences*, 19(3), pp.7-9.

8. Appendices

Appendix 1:

Lysogeny Broth LB Agar:

NaCl	10g
Tryptone	10g
Yeast Extract	5g
Agar No.2	15g
Distilled water (H_2O)	1000mL

Preparation: The nutrient mix was dissolved in 1000mL of distilled water, then autoclaved at 121^{o}C for 1 hour. The agar was then poured into petri dishes and allowed to set. The plates were then stored at 4^{o}C.

Chalkley's medium:

Stock in 1 Litre of distilled water

NaCl	20g
KCl	0.8g
$CaCl^2$	1.2g

Preparation: A 5mL aliquot of this stock solution to 995mL of distilled water and then autoclaved 121^{o}C for 1 hour. The diluted medium was then ready for *T. pyriformis* culture.

Blue Green 11 (BG11) Broth:

Stock: each per 500ml distilled water

Boric Acid (H_3BO_3)	2.86g
Manganese Chloride Tetrahydrate ($MnCl_2.4H_2O$)	1.81g
Zinc Sulphate heptahydrate ($ZnSO_4.7H_2O$)	0.22g
Sodium Molybdate Dihydrate ($Na_2MoO_4.2H_2O$)	0.39g
Copper Sulphate Pentahydrate ($CuSO_4.5H_2O$)	0.08g
Cobalt Nitrate Hexahydrate (Co $(NO_3)_2.6H_2O$	0.05g

A.	**Sodium Nitrate ($NaNO_3$)**	75g
B.	**Dipotassium phosphate (K_2HPO_4)**	2g
C.	**Magnesium Sulphate Heptahydrate ($MgSO_47H_2O$)**	3.75g
D.	**Calcium Chloride Dihydrate ($CaCl_2.2H_2O$)**	1.8g
E.	**Citric acid**	0.3g
F.	**Ammonium ferric citrate green**	0.3g
G.	**EDTANa2**	0.05g
H.	**Sodium Carbonate (Na_2CO_3)**	1g

Stock: Trace metals in 1000ml of distilled water

Preparation: A 10ml aliquot of the stock solutions A-H and 1ml aliquot of the stock solution I. were added to a flask, which was then topped up to 1000ml of distilled water. The pH. was kept to 7.1 with the addition of 1M Sodium hydroxide (NaOH) or Hydrochloric acid (HCl). Oxoid L11 agar was added (15g) and the medium was autoclaved at 121^oC for 1 hour.

Appendix 2

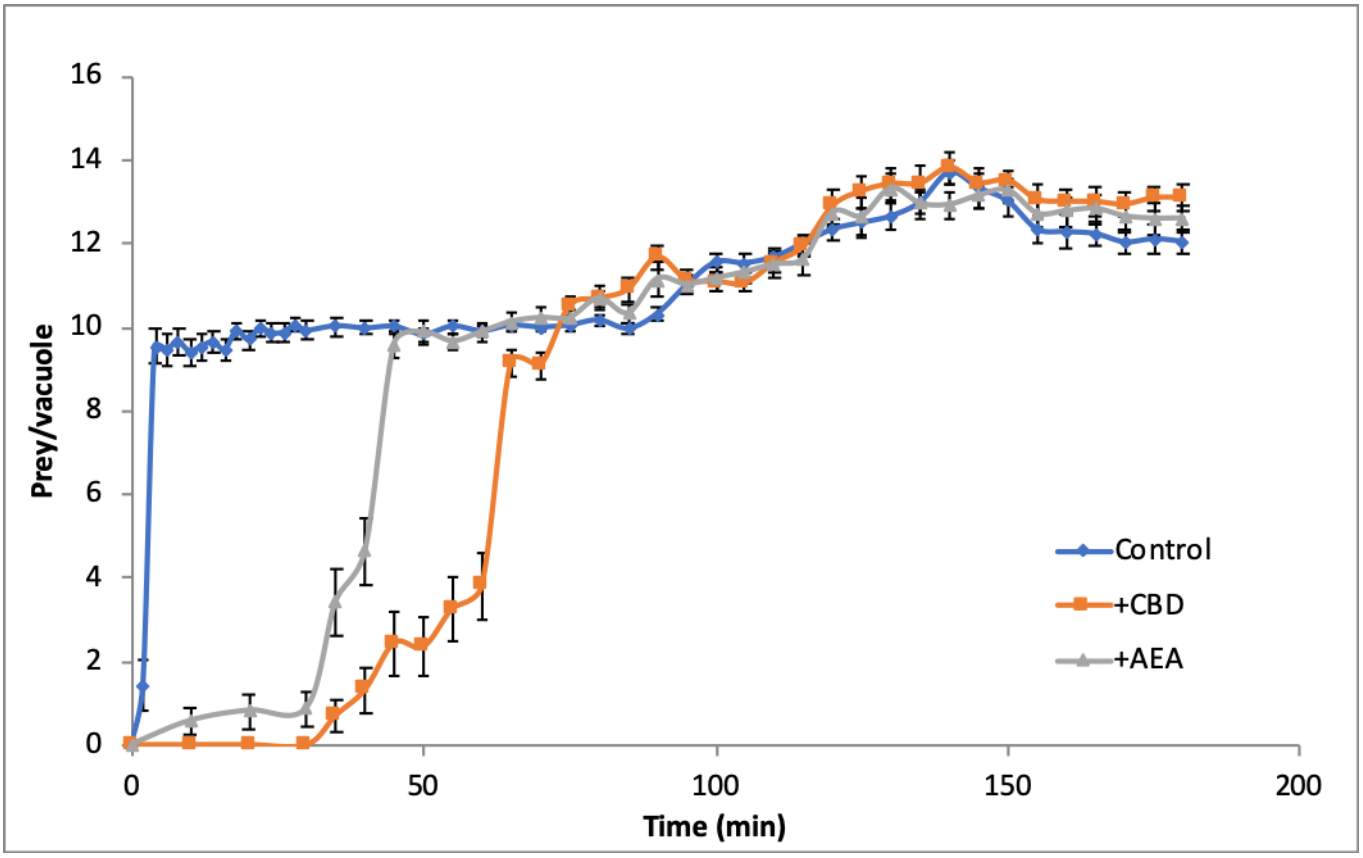

T. pyriformis was fed with *Synechococcus* at 1x10^7 cells/ml in the absence (Control) or presence of CBD and AEA (4µM). The average number (±SEM) of prey per vacuole. The experimental time was 180 minutes.